

Breaking the Data Barrier in Learning Symbolic Computation: A Case Study on Variable Ordering Suggestion for Cylindrical Algebraic Decomposition*

Rui-Juan Jing^{†a}, Yuegang Zhao^{†a}, Changbo Chen^{b,c}

^a*School of Mathematical Sciences, Jiangsu University, Zhenjiang, Jiangsu, China*

^b*Chongqing Institute of Green and Intelligent Technology, Chinese Academy of Sciences, Liangjiang New Area, Chongqing, China*

^c*Chongqing School, University of Chinese Academy of Sciences, Liangjiang New Area, Chongqing, China*

Abstract

Symbolic computation, powered by modern computer algebra systems, has important applications in mathematical reasoning through exact deep computations. The efficiency of symbolic computation is largely constrained by such deep computations in high dimension. This creates a fundamental barrier on labelled data acquisition if leveraging supervised deep learning to accelerate symbolic computation. Cylindrical algebraic decomposition (CAD) is a pillar symbolic computation method for reasoning with first-order logic formulas over reals with many applications in formal verification and automatic theorem proving. Variable orderings have a huge impact on its efficiency. Impeded by the difficulty to acquire abundant labelled data, existing learning-based approaches are only competitive with the best expert-based heuristics. In this work, we address this problem by designing a series of intimately connected tasks for which a large amount of annotated data can be easily obtained. We pre-train a Transformer model with these data and then fine-tune it on the datasets for CAD ordering. Experiments on publicly available CAD ordering datasets show that on average the orderings predicted by the new model are significantly better than those suggested by the best heuristic methods.

Keywords:

cylindrical algebraic decomposition, variable ordering, transformer, data scarcity, pre-training, fine-tuning

1. Introduction

The advent of deep learning and subsequent emergence of large language models (LLMs) have revolutionized the area of image and language processing and have been deeply impacting many areas in engineering and science. Despite of the decades advances in artificial intelligence (AI), efficient and robust reasoning remain a challenging task (Mitchell, 2025). For now, the logic and computation oriented approaches remain the dominant ones for trustworthy reasoning, powered respectively by proof assistants and computer algebra systems. Some efforts have been made to leverage the synergy between the learning-oriented and logic/computation-oriented approaches Lu et al. (2023). However, it remains a challenge to combine them towards more efficient and robust reasoning Xia et al. (2025).

Cylindrical algebraic decomposition (CAD) Collins (1975) is one of the main general approaches for performing quantifier elimination and reasoning with first-order logic formulas over reals Tarski (1998). Despite of the worst time complexity being doubly exponential Brown and Davenport (2007), its practical efficiency has been incrementally improved through numerous theoretical and algorithmic advances as well as various implementation efforts in independent packages or computer algebra systems, such as in QEPCAD Collins and Hong (1991); Brown (2003), Mathematica Strzebonski (2000), Redlog Seidl and Sturm (2003), Maple Chen and Moreno Maza (2014a), etc. The theoretical/algorithmic improvements haven been achieved in different ways, including incremental improvements to

*This work is supported by the National Key Research Project of China under Grant No. 2023YFA1009402, the National Natural Science Foundation of China under Grant No. 12101267 and Chongqing Talents Plan Youth Top-Notch Project (2021000263). Rui-Juan Jing (rjing@ujs.edu.cn) and Yuegang Zhao (ygzhao@stmail.ujs.edu.cn) contributed equally to the work. Corresponding author: Changbo Chen (chenchangbo@cigit.ac.cn).

Collins' original projection-lifting framework via improved projection operator [Hong \(1990\)](#); [Lazard \(1994\)](#); [McCallum \(1998\)](#); [Brown \(2001\)](#); [McCallum et al. \(2019\)](#), improved lifting [Strzebonski \(2006\)](#); [Iwane et al. \(2013\)](#), input formula aware partial cylindrical algebraic decomposition [Collins and Hong \(1991\)](#); [Bradford et al. \(2016\)](#), as well as more geometric ways through triangular decompositions [Chen et al. \(2009\)](#) and Gröbner bases [Chen \(2025\)](#).

In particular, it has become an indispensable part of satisfiability modulo theory (SMT) for non-linear arithmetic [Jovanovic and de Moura \(2012\)](#) and has been integrated into various SMT solvers [de Moura and Bjørner \(2008\)](#); [Dutertre \(2014\)](#); [Barbosa et al. \(2022\)](#); [Corzilius et al. \(2015\)](#), which in turn unleashed the potential of CAD on addressing problems of larger size as a local approach [Brown and Košta \(2015\)](#); [Li et al. \(2023b\)](#); [Nalbach et al. \(2024\)](#). There is no doubt that well-designed heuristics have played an important role in boosting the efficiency of SAT/SMT solvers. Recently, machine learning techniques have started to be integrated [Lu et al. \(2024\)](#) into them.

For cylindrical algebraic decomposition, as the variable ordering can significantly affect its efficiency, several heuristics have been proposed [Brown \(2004\)](#); [Dolzmann et al. \(2004\)](#); [Chen et al. \(2011\)](#); [Li et al. \(2023a\)](#); [del Rio Almajan and England \(2022\)](#); [Pickering et al. \(2024a\)](#). Currently, the heuristics perform much better than random choices, but are still far away from the optimal ordering [Chen et al. \(2020, 2024\)](#). The huge room for improvement have attracted several attempts to utilize machine learning to suggest better variable orderings, reviewed in Section 2. These learning-oriented models have demonstrated the potential to surpass the heuristic methods designed by experts, but the lead is minor in general. In fact, the Transformer model [Vaswani et al. \(2017\)](#), initially invented for natural language processing, has been used in [Chen et al. \(2024\)](#) for the CAD ordering selection problem. However, it does not noticeably surpass other models or the heuristic methods.

On the other hand, Transformer has found applications in learning some other tasks related to symbolic computation. Existing work mainly fall into two groups. The first group of work focus on end-to-end learning a simple output from a simple input for complex tasks, such as symbolic integration [Lample and Charton \(2020\)](#), computing Lyapunov functions [Alfarano et al. \(2024\)](#), computing Gröbner bases [Kera et al. \(2024\)](#), etc. The second group of work focus on understanding the limitation and power of Transformer architecture on learning basic arithmetic operations like integer addition and multiplication [Quirke and Barez \(2024\)](#); [Lee et al. \(2024\)](#); [McLeish et al. \(2024\)](#). Surprisingly, these “basic tasks” are not necessarily easier to learn than “complex tasks”. In this work, we are interested to explore the power of Transformer to learn better strategies to replace existing heuristic ones used in the computation of complex tasks. For the above mentioned work, we note that what is in common for successful learning is that: (i) a huge/large amount of labelled data are available, by either a forward or a backward process, for training Transformer models; (ii) both input and output must be relatively simple expressions.

In the case of selecting variable orderings for CAD, we do not know an economic way to synthesize the data. At present, to create the correct label for the input system, one has to construct CADs for all possible orderings and pick the best one according to either the minimal time or the least number of cells. Hence, regards CAD ordering, even both the input system and the output ordering are simple expressions, the ordering selection task itself should be treated as a complex one as it involves conducting a complex computation task. The complex nature of this task also implies the data scarcity. Indeed, in [Chen et al. \(2024\)](#), building a dataset of size 20K costs more than 140 CPU days. This makes CAD ordering a good case study for leveraging deep learning for complicated symbolic computation in the circumstance of data scarcity.

The proposed approach is to leverage the pre-training and fine-tuning paradigm to address the data scarcity problem for CAD ordering selection. More precisely, our main contribution in this work is three-fold:

- We propose several simple pre-training tasks intimately connected to CAD. By generating large random datasets for them, we pre-train Transformer models for these tasks to achieve reasonable performance.
- We design a pre-training & fine-tuning framework to leverage the pre-trained models to help learning the variable ordering selection task. We explain our choices through intensive ablation analysis.
- We enhance a public four variables random dataset [Chen et al. \(2024\)](#) for CAD variable ordering selection (the new labelled data cost about 36 days to generate) and make the new dataset publicly available at <https://doi.org/10.57760/sciencedb.31989>. We conduct experiments on public random datasets for three and four variables as well as a real dataset originated from benchmarks for satisfiability modulo theory (SMT) solvers.

2. Related work on learning the optimal variable ordering for CAD

In this section, we briefly review existing works on variable ordering selection for cylindrical algebraic decomposition and explain how they motivate the present work.

The first work [Huang et al. \(2014\)](#) applies machine learning to choose the best heuristic method from several candidates. The learned one outperforms each individual, but the performance is also limited by the best heuristic. The work [England and Florescu \(2019\)](#) and [Zhu and Chen \(2020\)](#) propose classification models to directly choose the best variable ordering respectively according to the running time and number of cells by expanding features used in heuristic methods in different ways. As the number of possible variable orderings is $n!$ for n variables, direct classification models would be infeasible for large n in terms of data acquisition and classification.

To overcome this problem, the work [Chen et al. \(2020\)](#) proposes an iterative method IVO with quadratic complexity to explore the variable ordering space to find orderings performing much better than the heuristic one. Like the earlier iterative approach sotd [Dolzmann et al. \(2004\)](#) and the latter proposed heuristic mod [del Rio Almajan and England \(2022\)](#), it involves heavy CAD computation and cannot predict the variable ordering on the fly. In the same paper, they propose an approach PVO learning to predict only the leading variable in the ordering, which is then used to rotate an initial variable ordering suggested by a heuristic method. This approach relies on the same graph features proposed in [Zhu and Chen \(2020\)](#).

Later, it is realized in both [Jia et al. \(2023\)](#) and [Jing et al. \(2024\)](#) that the CAD ordering selection could be modelled as a Markov decision process and the reinforcement learning approaches naturally applies. Instead of making a $n!$ -classification to select an ordering, it suffices to take a sequence of $n - 1$ actions and each action only needs to make at most $n - i$ different choices at step i , $i = 0, \dots, n - 1$. The work [Jia et al. \(2023\)](#) is only trained on random datasets with 3 variables and its generalization ability on datasets with more variables is limited. The work [Jing et al. \(2024\)](#) achieves significant speedup for systems up to 16 variables but is limited to systems with the same support. The limitation of these learning based methods further motivates the work [Pickering et al. \(2024a\)](#) to leverage explainable AI to propose better heuristics (see independent evaluations in [Chen et al. \(2024\)](#)).

In summary, we have the following observations on the variable ordering problem for CAD: (i) the potential for accelerating CAD computation by choosing an optimal variable ordering is huge and such potential is only exploited in a moderate level; (ii) the existing approaches that further exploit the deep features of projected polynomials, not matter heuristic or learning oriented, could outperform the ones that utilize only the shallow features of input systems; (iii) the ones that further exploit the deep features of projected polynomials cannot suggest the variable ordering on the fly as they all have to explicitly compute projected polynomials; (iv) it is difficult, if not impossible, to generate a huge dataset for the CAD ordering selection problem. Although data augmentation by permuting variables can increase the dataset size for free, it brings limited benefit on the model's performance [Hester et al. \(2023\)](#); [del Río Almajan and England \(2023\)](#). Based on these observations, we view CAD ordering as a complex task featured with data scarcity and propose to apply the pre-training and fine-tuning paradigm to solve this problem.

3. Cylindrical algebraic decomposition

In this section, we briefly recall the notion of cylindrical algebraic decomposition.

Let $F \subset \mathbb{Q}[x_1, \dots, x_n]$ and let $x_1 < \dots < x_n$ be a given variable ordering. An F -invariant CAD, w.r.t. the ordering $x_1 < \dots < x_n$, decomposes \mathbb{R}^n into finitely many connected semi-algebraic sets, called cells, such that these cells form a cylindrically arranged partition of \mathbb{R}^n , namely the projections of any two cells onto any \mathbb{R}^i , $i = 1, \dots, n - 1$ are either identical or disjoint. Moreover, above each cell, the polynomials in F enjoy some invariant property, such as sign invariant or order invariant.

Let $F_n := \{f \mid f \in F, \text{mvar}(f) = x_n\}$ and $F_o = F \setminus F_n \subset \mathbb{Q}[x_1, \dots, x_{n-1}]$. Here $\text{mvar}(f)$ denotes the largest variable appearing in f according to a given variable ordering. Let F_s be a squarefree basis of F_n . The original idea of Collins for computing an F -invariant CAD is to find a projection operator which maps F_s into another finite set of polynomials $F_p \subset \mathbb{Q}[x_1, \dots, x_{n-1}]$, such that an F -invariant CAD C_n of \mathbb{R}^n can be constructed from an $F_p \cup F_o$ -invariant CAD C_{n-1} of \mathbb{R}^{n-1} by building a stack of cells of \mathbb{R}^n above each cell of C_{n-1} .

In this work, we are based on the Maple built-in command (since Maple 2020) `CylindricalAlgebraicDecompose` [Chen and Moreno Maza \(2014c\)](#) inside the `RegularChains` library (denoted by RC-CAD for short) for computing CADs. This command implements the triangular decomposition based algorithms for computing a CAD [Chen et al.](#)

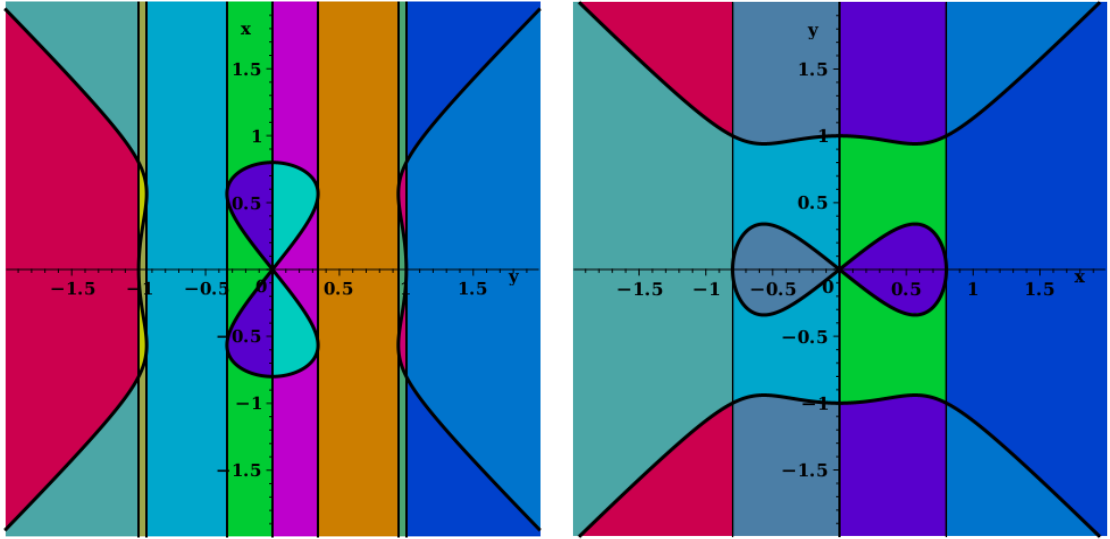


Figure 1: CADs of the Devil’s curve under the ordering $x > y$ and $y > x$.

(2009); [Chen and Moreno Maza \(2014b\)](#). More precisely, given a system of polynomial equations and inequalities, say $\text{sys} := \{f_1 = \dots = f_m = 0, g_1 > 0, \dots, g_s > 0\}$, it first computes a special triangular decomposition, called cylindrical decomposition \mathcal{D} of the zero set of $\text{sys} := \{f_1 = \dots = f_m = 0, g_1 \neq 0, \dots, g_s \neq 0\}$ in \mathbb{C}^n such that the cells of \mathcal{D} are cylindrically arranged. If a set of polynomials F is given, it computes a cylindrical decomposition \mathcal{D} of \mathbb{C}^n such that above each cell of \mathcal{D} , each polynomial in F either vanishes at all points of the cell or vanishes at no points of the cell. To obtain a cylindrical algebraic decomposition, it further refines each cell in the cylindrical decomposition into a disjoint union of cylindrically arranged connected semi-algebraic sets via real root isolation of regular chains.

Although the projection-lifting scheme and the triangular decomposition scheme compute CAD following different philosophy, they share many common operations in the specific algorithms implementing the philosophy, especially when the input is a pure set of polynomials or has no equational constraints. Let $F \subset \mathbb{Q}[x_1, \dots, x_n]$. For simplicity, one could first compute a union of irreducible factors of polynomials in F , denoted by G . Let $x_1 < \dots < x_n$ be a given variable ordering. For most of the algorithms implementing both the two schemes, if no equational constraints are present, they all need to carry at least the following computations. Let $G_n := \{g \mid g \in G, \text{mvar}(g) = x_n\}$ and $G_o = G \setminus G_n$. Let $E_{n-1} := \{\text{lc}(g, x_n) \mid g \in G_n\} \cup \{\text{discrim}(g, x_n) \mid g \in G_n\} \cup \{\text{res}(g, h, x_n) \mid g \in G_n, h \in G_n, g \neq h\}$. Here $\text{lc}(g, x_n)$, $\text{discrim}(g, x_n)$, and $\text{res}(g, h, x_n)$ denote respectively the leading coefficient of g , the discriminant of g , and the resultant of g and h w.r.t. the variable x_n . We call $\text{pf}(F, x_n) := \{g \mid g \in G_o \cup E_{n-1}, g \notin \mathbb{Q}\}$ the *first projection factor set* of F under the variable ordering $x_1 < \dots < x_n$.

Example 1. Let $f := y^2(y^2 - b^2) - x^2(x^2 - a^2)$. For fixed values of a and b , its zero set in \mathbb{R}^2 defines a Devil’s curve. Let $a = 4/5$, $b = 1$, $g = 25f$, and $F := \{g\}$. Then an F -sign invariant CAD under the order $x > y$ (resp. $y > x$) is illustrated by the left (resp. right) subfigure of Fig 1. The number of CAD cells in the left (resp. right) subfigure is 89 (resp. 49).

4. Method

In this section, we introduce a Transformer-based framework to tackle the problem of variable ordering selection for CAD by leveraging a pre-training and fine-tuning paradigm.

Pre-training and fine-tuning is a learning paradigm popularized by the encoder-only Transformer model BERT [Devlin et al. \(2019\)](#). It represents a specific form of transfer learning [Wang and Chen \(2023\)](#), well suited for tackling complex learning tasks under limited data availability. Originally used for natural language processing, the core idea

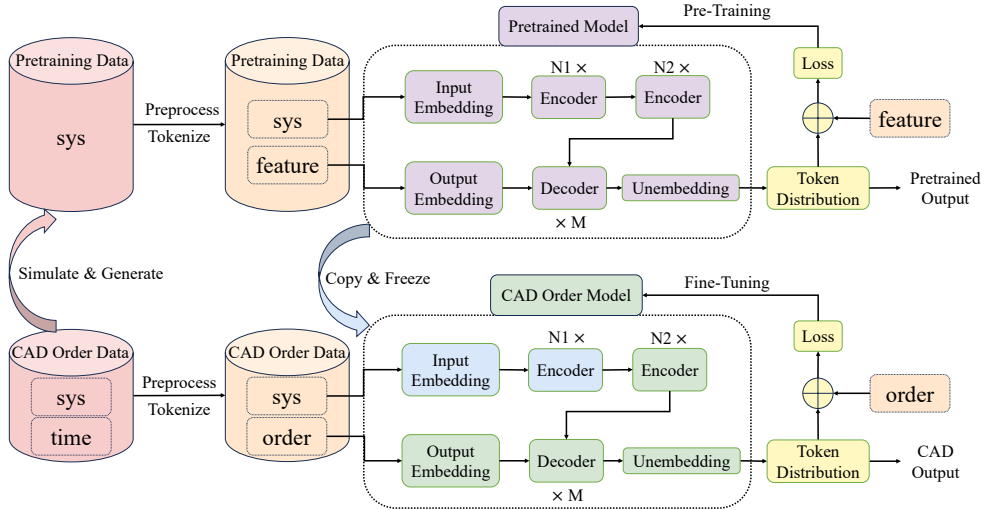


Figure 2: An overview of the proposed framework for CAD variable ordering selection.

is to pre-train a model to “understand” the input language or have a good representation of the input language by utilizing the contextual information. In general, pre-training can be used in the situation where huge amount of labelled data are accessible for training a model to learn a common representation/embedding which might be useful for many downstream tasks. Fine-tuning, on the other hand, can inherit such a common representation and may keep refining it for a particular downstream task.

In our context, the main task is to train a model to effectively predict the variable ordering for CAD. However, we only have limited labelled data for this task. To leverage the power of the pre-training and fine-tuning paradigm, we have to create suitable pre-training tasks such that on one hand these tasks are closely related to the main task and on the other hand collecting a large amount of data for these pre-training tasks should be relatively easy. Section 4.1 provides an overview of the framework. The pre-training tasks are detailed in Section 4.3. Some of these tasks are inspired by the features used in heuristic methods for variable ordering selection, which are recalled in Section 4.2. The process for generating the labelled dataset for each task is detailed in Section 4.4. These data have to be tokenized to be used with the Transformer models. The tokenization scheme is elaborated in Section 4.5.

4.1. The framework for CAD variable ordering selection

An overview of the proposed pre-training and fine-tuning framework for CAD variable ordering selection is illustrated by Figure 2. The entire process begins with generating a large number of random systems that reflect the structural characteristics of those in the CAD order dataset, including the number of constraints, the number of variables, and the exponents of variables. Each generated system is then preprocessed to extract a feature vector, which serves as its label according to a designed pre-training task. The resulting labeled dataset is subsequently tokenized and used to train and evaluate a Transformer model. The model obtained through this pre-training procedure is referred to as the *pre-trained model*.

After pre-training, we fine-tune the model on the CAD order dataset. During fine-tuning, we freeze the input embedding layers and some early encoder layers (highlighted in light blue in Figure 2). These layers are expected to encode task-independent structural properties of input systems, as well as basic computational behaviors that facilitate learning effective variable orderings for CAD construction. The remaining unfrozen layers are then trained using the CAD order dataset, enabling the model to specialize in CAD variable ordering prediction. This fine-tuning strategy allows the model to leverage the general representations learned during pre-training while adapting to the specific patterns of the downstream task.

4.2. Important features relevant to the variable ordering

Let $F \subset \mathbb{Q}[x_1, \dots, x_n]$. For any polynomial $f \in F$ and any variable $v \in \{x_1, \dots, x_n\}$, we can write f as a sum of distinct terms $f = \sum_i T_i = \sum_i c_i \prod_{j=1}^n x_j^{d_{ij}}$, where each coefficient $c_i \neq 0$. Let \mathcal{T}_f denote the set of all terms of f . For a term $T_i \in \mathcal{T}_f$, its *degree* with respect to $v = x_j$ is defined as d_{ij} , and is denoted by $\mathbf{d}(T_i, v)$. The total degree of T_i is $\sum_{j=1}^n d_{ij}$. The variable $v = x_j$ occurs in T_i if and only if $d_{ij} \neq 0$. For a given term $T \in \mathcal{T}_f$, define $\mathbf{a}(T, v) = 1$ if v appears in T and $\mathbf{a}(T, v) = 0$ otherwise. The *effective total degree* of T w.r.t. v , denoted by $\mathbf{e}(T, v)$, is the total degree of T if v appears in T and 0 otherwise. Denote $\mathbf{d}(F, v) := \{\{\mathbf{d}(T, v) \mid T \in \mathcal{T}_f\} \mid f \in F\}$, $\mathbf{a}(F, v) := \{\{\mathbf{a}(T, v) \mid T \in \mathcal{T}_f\} \mid f \in F\}$, and $\mathbf{e}(F, v) := \{\{\mathbf{e}(T, v) \mid T \in \mathcal{T}_f\} \mid f \in F\}$. In the above definition, each $\mathbf{d}, \mathbf{a}, \mathbf{e}$ can be seen as an operator which takes F and v as input and returns a set of rational numbers.

Let $S := \{S_1, \dots, S_t\}$ be a finite nonempty collection of sets, where each S_i is a nonempty finite set of rational numbers. Let $R := \{R_1, \dots, R_r\}$ be a finite set of *reduction operations*, where each R_j is a mapping that takes a set as input and returns a rational number. For any $i, j \in \{1, \dots, r\}$, we define a *composite reduction operation* $R_i \circ R_j(S) := R_i(\{R_j(S_1), \dots, R_j(S_t)\})$. Typical examples of reduction operations include *sum*, which computes the sum of all elements in a set; *avg*, which computes the average; and *max* (resp. *min*), which returns the maximum (resp. minimum) element. Given a finite set $F \subset \mathbb{Q}[x_1, \dots, x_n]$, a variable $v = x_i$, an operator o in $\{\mathbf{d}, \mathbf{a}, \mathbf{e}\}$, and two reduction operations Rf and Rs in R , we can then define a feature operator $Rs \circ Rf \circ o(F, v) := Rs \circ Rf(o(F, v))$. The relation between our notations and the ones in [Pickering et al. \(2024b\)](#) is as follows: $\mathbf{d} = "v"$, $\mathbf{a} = "sg_v"$ and $\mathbf{e} = "sv"$.

In Table 5 of [Pickering et al. \(2024b\)](#), with the SHAP (SHapley Additive exPlanations) method, 27 different feature operators are selected. Since the reduction operation *avg* introduces rational numbers, causing extra difficulty for learning with Transformer, we only keep 11 of them. Moreover, since *max_max_a* would always be 1 if a variable appears in the input polynomials, we replace it with *sum_max_a*. This results in the following 11 feature operators:

sum_max_d, sum_max_e, sum_sum_d, sum_sum_e, sum_sum_a, max_max_d,
max_sum_e, max_max_e, sum_max_a, max_sum_d, max_sum_a.

4.3. Pre-training tasks

We denote by `task_c` the task of predicting the optimal variable ordering for CAD. The precise meaning of “optimal” will be made clear in Section 4.4. As generating a large amount of labelled data for this task is very challenging, we would define a series of pre-training tasks relevant to `task_c`. For these pre-training tasks, it is much easier to obtain abundant labelled data.

In Subsection 4.2, we introduced 11 feature operators. For a polynomial set F in n variables, applying them to F w.r.t. each variable generates a feature vector of length 11. Concatenating these n individual vectors forms the ie_{11} feature vector of F . These features have been shown to be effective in both heuristic and learning-oriented approaches for selecting the variable ordering of CAD. We then denote by `task_f` the pre-training task for predicting the ie_{11} features of F . As recalled in Section 3, most of the algorithms for computing CAD involve computing at least the first level projection factor set $pf(F, x_i)$ for a given variable ordering with x_i being the leading one. The ie_{11} features of $\bigcup_{i=1}^n pf(F, x_i)$ include degree and other important information on these projection factor sets. Thus, it is reasonable to list it as a pre-training task, denoted by `task_p`.

Let p be the squarefree part of the product of all polynomials in F , and let $v \in \{x_1, \dots, x_n\}$. The set of irreducible factors of $r_v := \text{res}(p, v)$ coincides with the union of the irreducible factors of the polynomials in $pf(F, v)$. Let sr_v denote the squarefree part of r_v . We construct a feature vector of length 4 consisting of the total degree of r_v , the total degree of sr_v , the number of terms in r_v , and the number of terms in sr_v . By concatenating the n such vectors, we obtain the re_4 feature vector of F . The pre-training task corresponding to predicting re_4 is referred to as `task_r`. Table 1 summarizes the main task `task_c` together with all its pre-training tasks.

Next, we use Example 2 to illustrate the tasks presented in Table 1. Note that for `task_f`, `task_m`, `task_p`, `task_r` and `task_s`, the corresponding feature vector can be reshaped as a feature matrix $M_{d \times n}$, where d is the number of feature operators applied and n is the number of variables. Flattening the matrix in column-major order recovers the feature vector in the definition. Flattening the matrix in row-major order gets the feature vector actually implemented. In Example 2, the feature vector is displayed in row-major order.

Table 1: Description of the training tasks.

Task	Description
task_c	Predict the optimal variable ordering for CAD.
task_e	Predict the exponent vectors of input polynomials.
task_f	Predict the ie_{11} feature vector of the set of input polynomials F .
task_m	Predict the exponent vectors of the product of input polynomials.
task_p	Predict the ie_{11} feature vector of $\bigcup_{i=1}^n pf(F, x_i)$.
task_r	Predict the re_4 feature vector of F .
task_s	Predict the ie_{11} feature vector of $\bigcup_{i=1}^n pf(\{p\}, x_i)$, where p is the square-free part of the product of polynomials in F .

Example 2. Let $f_1 = -6x_1^3x_2 - 4x_1x_2x_3^2 + 2x_2^2x_3 + 1$ and $f_2 = -5x_3^4 + x_3^3 - 7$ be two polynomials in variables x_1, x_2, x_3 . Let $F := \{f_1, f_2\}$ and $sys := \{f_1 = 0, f_2 = 0\}$. The system sys and the timings for computing a CAD for it under different variable orderings are taken from the dataset DQ-3 in [Chen et al. \(2024\)](#).

task_c. The six variable orderings, $\{[x_1, x_2, x_3], [x_1, x_3, x_2], [x_2, x_1, x_3], [x_2, x_3, x_1], [x_3, x_1, x_2], [x_3, x_2, x_1]\}$, with the corresponding CAD running times (in seconds) $\{0.035, 0.080, 0.034, 0.048, \text{timeout}, \text{timeout}\}$, where the time limit was set as 900 seconds. The absolute optimal ordering, i.e. the one yielding the shortest running time, is

$$\mathbf{best_order} := [x_2, x_1, x_3].$$

task_e. We have $\mathcal{T}_{f_1} = \{-6x_1^3x_2, -4x_1x_2x_3^2, +2x_2^2x_3, +1\}$ and $\mathcal{T}_{f_2} = \{-5x_3^4, +x_3^3, -7\}$, discarding constant terms, yielding the exponent vectors:

$$\mathbf{feature_e} := \{[(3 \ 1 \ 0); (1 \ 1 \ 2); (0 \ 2 \ 1)], [(0 \ 0 \ 4); (0 \ 0 \ 3)]\}.$$

task_f. As $\mathbf{d}(F, x_1) := \{\{3, 1, 0, 0\}, \{0, 0, 0\}\}$, $\mathbf{d}(F, x_2) = \{\{1, 1, 2, 0\}, \{0, 0, 0\}\}$, and $\mathbf{d}(F, x_3) = \{\{0, 2, 1, 0\}, \{4, 3, 0\}\}$, we have $\text{sum_max_d}(F, x_1) = 3$, $\text{sum_max_d}(F, x_2) = 2$, and $\text{sum_max_d}(F, x_3) = 6$, yielding the first feature vector $(3 \ 2 \ 6)$. The rest can be deduced in a similar way, producing the ie_{11} features:

$$\mathbf{feature_f} := [(3 \ 2 \ 6); (4 \ 4 \ 8); (4 \ 4 \ 10); (8 \ 11 \ 14); (2 \ 3 \ 4); (3 \ 2 \ 4); (8 \ 11 \ 7); (4 \ 4 \ 4); (1 \ 1 \ 2); (4 \ 4 \ 7); (2 \ 3 \ 2)].$$

task_m. The exponent vectors of the product of f_1 and f_2 are:

$$\mathbf{feature_m} := [(3 \ 1 \ 4); (1 \ 1 \ 6); (3 \ 1 \ 3); (1 \ 1 \ 5); (0 \ 2 \ 4); (3 \ 1 \ 0); (1 \ 1 \ 2); (0 \ 0 \ 4); (0 \ 2 \ 1); (0 \ 0 \ 3)].$$

task_p. As $\bigcup_{i=1}^3 pf(F, x_i) = \{5x_3^4 - x_3^3 + 7, 6x_2, -1536x_2^4x_3^6 - 3888x_2^6x_3^2 - 3888x_2^4x_3 - 972x_2^2, 5x_3^4 - x_3^3 + 7, -2x_3, 36x_1^6 + 48x_1^4x_3^2 + 16x_1^2x_3^4 - 8x_3, 4x_1x_2, -96x_1^4x_2^2 + 4x_2^4 + 16x_1x_2, 32400x_1^{12}x_2^4 + 864x_1^{10}x_2^4 - 2160x_1^9x_2^5 - 21600x_1^8x_2^3 + 40320x_1^8x_2^4 - 432x_1^7x_2^3 + 1080x_1^6x_2^4 + 4032x_1^5x_2^5 - 13440x_1^4x_2^6 + 5400x_1^6x_2^2 - 13440x_1^5x_2^3 + 12544x_1^4x_2^4 - 224x_1x_2^7 + 560x_2^8 + 72x_1^4x_2^2 - 180x_1^3x_2^3 - 672x_1^2x_2^4 + 2240x_1x_2^5 - 600x_1^3x_2 + 1120x_1^2x_2^2 - 4x_1x_2 + 10x_2^2 + 25\}$, we have

$$\mathbf{feature_p} := [(23 \ 20 \ 19); (30 \ 35 \ 25); (120 \ 107 \ 31); (202 \ 224 \ 51); (26 \ 31 \ 11); (12 \ 8 \ 6); (174 \ 184 \ 23); (16 \ 16 \ 10); (4 \ 5 \ 5); (102 \ 82 \ 9); (20 \ 22 \ 3)].$$

task_r. Let p be the squarefree part of the product of polynomials in F . Let $v = x_1$, we have $r_v := \text{res}(p, v) = 72x_2^3(128x_2^2x_3^6 + 324x_2^4x_3^2 + 324x_2^2x_3 + 81)(5x_3^4 - x_3^3 + 7)^5$. Thus the total degree of r_v is 31, and the total degree of the squarefree part sr_v of r_v is 13. The result can be obtained in a similar way, yielding the re_4 features:

$$\mathbf{feature_r} := [(31 \ 19 \ 40); (13 \ 11 \ 23); (60 \ 40 \ 144); (12 \ 12 \ 45)].$$

task_s. Computing $\bigcup_{i=1}^3 pf(\{p\}, x_i)$ brings six polynomials $\{6x_2(5x_3^4 - x_3^3 + 7), -960000x_2^4x_3^{22} + \dots, -2x_3(5x_3^4 - x_3^3 + 7), 900x_1^6x_3^8 + \dots, 20x_1x_2, -1105994585041920000x_1^{28}x_2^{10} - \dots\}$, yielding the following ie_{11} features:

$$\mathbf{feature_s} := [(35 \ 28 \ 43); (54 \ 71 \ 50); (1506 \ 1643 \ 703); (3010 \ 3616 \ 961); (157 \ 196 \ 75); (28 \ 20 \ 22); (2816 \ 2880 \ 722); (38 \ 38 \ 26); (3 \ 4 \ 4); (1433 \ 1447 \ 532); (138 \ 144 \ 47)].$$

4.4. Preprocessing the data

In this section, we detail the preprocessing pipeline applied to the raw datasets used in this work, which include both the CAD data and the pre-training data. The goal is to articulate how these two types of data are transformed from their initial raw forms into structured inputoutput pairs suitable for model learning.

For raw CAD data, each instance is represented as an inputoutput pair $(\text{sys}, \text{time})$, where sys denotes an n -variable polynomial system and time records the running timings of the CAD solver under all $n!$ possible variable orderings. Let t^* denote the minimum running time. Extensive empirical evidence indicates that certain orderings, while not attaining the exact minimum, yield running timings that are nearly indistinguishable from t^* . To capture these cases, we introduce a tolerance parameter $\tau = 0.03$ and define the set of relative optimal orderings as $O_{\text{rel}} = \{ \text{order} \mid t(\text{order}) \leq (1 + \tau) t^* \}$. For convenience, unless otherwise stated, the term “optimal” is used to refer to any ordering within O_{rel} , thereby subsuming the absolute optimum as a special case. For instance, in Example 2, with $\tau = 0.03$, both $[x_2, x_1, x_3]$ and $[x_1, x_2, x_3]$ are considered to be optimal. The objective of preprocessing raw CAD data is to transform each instance into pairs of the form $(\text{sys}, \text{optimal_order})$.

The raw pre-training data consist of only the input polynomial systems. The objective of preprocessing in this setting is to construct inputoutput pairs of the form $(\text{sys}, \text{feature})$, where feature denotes the task-specific feature vector described in Table 1. The preprocessing step also includes a data screening procedure, detailed in Section 5.1.

Next, we clarify two subtle considerations regarding the CAD data preprocessing: (i) For both the training and validation datasets, the *absolute optimal ordering* is used as the target label. It may happen that multiple orderings yield the identical minimum running time. To accommodate this, we apply a multi-label strategy: if a system sys admits two absolute optimal orderings order_1 and order_2 , we record two separate samples $(\text{sys}, \text{order}_1)$ and $(\text{sys}, \text{order}_2)$. (ii) Since testing-validation and testing datasets are only used for prediction, no multi-label augmentation preprocessing on the data is applied. Instead, we assess the quality of evaluation under two complementary metrics: *absolute accuracy* (probability of predicting an absolute optimal ordering) and *relative accuracy* (probability of predicting a relative optimal ordering).

4.5. The tokenization scheme

To encode a CAD problem into a sequential format, we construct a specialized token set tailored for polynomial systems, encompassing both input and output sequence components. Table 2 presents the complete token vocabulary, organized into seven categories, used for n -dimensional CAD variable ordering selection problems in our study.

Table 2: The vocabulary of tokens.

Category	Tokens	Category	Tokens
Special tokens	$\langle s \rangle$ $\langle /s \rangle$ $\langle \text{pad} \rangle$	Separators	$\langle \text{sep} \rangle$; ,
Variables x_1, \dots, x_n	x_1, \dots, x_n	Digits of exponents	0–9
Arithmetic operators	$+ - * \wedge$	Digits of coefficients	c0–c9
Relational operators	$= > \geq < \leq \neq$	Digits of feature vectors	0–9

In the table, three special control symbols are introduced to facilitate sequence modeling: $\langle s \rangle$ marks the start of a sequence, $\langle /s \rangle$ denotes its termination, and $\langle \text{pad} \rangle$ serves as a padding placeholder for sequence alignment during batch processing. To further ensure structural clarity, three types of separators are defined: the comma ,? separates (features of) different polynomials in the same polynomial system, the semicolon ;? distinguishes different types of output features in pre-training tasks, and $\langle \text{sep} \rangle$ separates the n values associated with a single feature, thereby supporting a hierarchical and unambiguous representation.

For both exponents and feature vectors, we encode each digit of them separately. In contrast, the digits in the coefficients are prefixed with the letter “c” yielding $c_0 \dots c_9$. This strategy is adopted for two reasons: (i) the feature vectors are constructed based on the exponents of input/computed polynomials; (ii) exponents play a much more important role than coefficients in variable ordering selection, and it is desirable to distinguish their digits explicitly.

Furthermore, to enable the pre-training task to more effectively capture the structural features of polynomial systems, a completion procedure is applied to each polynomial term. Specifically, if a variable is absent, it is explicitly represented with an exponent of zero; similarly, variables of degree one are explicitly represented with an exponent of one. For example, in a system with three variables $\{x_1, x_2, x_3\}$, the term $-2x_2^2x_3$ is encoded as $\{ -, \text{c2}, *, \text{x1}, \wedge, 0, *\}$

$x_2, \wedge, 2, *, x_3, \wedge, 1\}$. In contrast, the encoding method in [Chen et al. \(2024\)](#) neither explicitly distinguishes between coefficients and exponents nor fully encodes the polynomial term (e.g. variables with zero exponents are omitted). Its encoded result for the same example is $\{ -, 2, *, x_2, \wedge, 2, *, x_3\}$.

During model training, sequences shorter than the maximum length within a batch are padded with $\langle \text{pad} \rangle$ tokens appended to their end until they match the batchs longest sequence, whereas sequences already at the maximum length remain unchanged without any padding.

Example 3. Next, we illustrate the encoding scheme in detail through tokenizing the polynomial system $\text{sys} := \{-6x_1^3x_2 - 4x_1x_2x_3^2 + 2x_2^2x_3 + 1 = 0, -5x_3^4 + x_3^3 - 7 = 0\}$ and its outputs for different tasks presented in [Example 2](#).

The sequence of tokens representing the input system sys is given as $\{\langle s \rangle, -, c6, *, x1, \wedge, 3, *, x2, \wedge, 1, *, x3, \wedge, 0, -, c4, *, x1, \wedge, 1, *, x2, \wedge, 1, *, x3, \wedge, 2, +, c2, *, x1, \wedge, 0, *, x2, \wedge, 2, *, x3, \wedge, 1, +, c1, =, c0, , -, c5, *, x1, \wedge, 0, *, x2, \wedge, 0, *, x3, \wedge, 4, +, x1, \wedge, 0, *, x2, \wedge, 0, *, x3, \wedge, 3, -, c7, =, c0, \langle /s \rangle\}$. The tokenization of an output ordering $[x_2, x_1, x_3]$ is simply $\{\langle s \rangle, x2, x1, x3, \langle /s \rangle\}$.

The tokenization of feature_e is given as $\{\langle s \rangle, 3, \langle \text{sep} \rangle, 1, \langle \text{sep} \rangle, 0, ;, 1, \langle \text{sep} \rangle, 1, \langle \text{sep} \rangle, 2, ;, 0, \langle \text{sep} \rangle, 2, \langle \text{sep} \rangle, 1, , 0, \langle \text{sep} \rangle, 0, \langle \text{sep} \rangle, 4, ;, 0, \langle \text{sep} \rangle, 0, \langle \text{sep} \rangle, 3, \langle /s \rangle\}$. It is important to note that while semicolon “;” are used to separate features, comma “,” are employed to distinguish different polynomial systems. As a result, both semicolons and commas may appear simultaneously in this pre-training task.

The tokenization of the other features are similar. Note that “,” will not appear in them and integers with multiple digits have to be separated into different tokens. For instance, feature_r is represented as $\{\langle s \rangle, 3, 1, \langle \text{sep} \rangle, 1, 9, \langle \text{sep} \rangle, 4, 0, ;, 1, 3, \langle \text{sep} \rangle, 1, 1, \langle \text{sep} \rangle, 2, 3, ;, 6, 0, \langle \text{sep} \rangle, 4, 0, \langle \text{sep} \rangle, 1, 4, 4, ;, 1, 2, \langle \text{sep} \rangle, 1, 2, \langle \text{sep} \rangle, 4, 5, \langle /s \rangle\}$.

5. Datasets

In this section, we present the datasets used in the experiments. In [Section 5.1](#), we firstly recall two public CAD variable ordering datasets DQ-3 and DQ-4 introduced in [Chen et al. \(2024\)](#) and then present how to generate pre-training datasets from them. In [Section 5.2](#), we introduce a new four variables dataset for CAD variable ordering selection. This new dataset DQ-4b enhances DQ-4 in [Section 5.1](#) by incorporating more difficult examples to improve its quality. In [Section 5.3](#), we recall an existing three variables CAD variable ordering dataset built with SMT examples [del Rio Almajan and England \(2022\)](#).

5.1. Two public random CAD variable ordering datasets and the corresponding pre-training datasets

The objective of this study is to train machine learning models to improve the accuracy of variable order prediction in CAD. To this end, high-quality CAD random datasets are required to evaluate model performance. The work in [Chen et al. \(2024\)](#) provides two benchmark datasets, DQ-3 and DQ-4, corresponding to three-variables and four-variables settings, respectively. These datasets contain polynomial systems along with the associated CAD running time under different variable orders.

Table 3: Two random CAD order datasets from [Chen et al. \(2024\)](#).

Dataset	Names of Sub-datasets
DQ-3	REcMdMn2p0tMv3, REcMeEn2p0rCv3, REcMeEn2tMv3, REdEn4rCv3, REdEn5rCv3, REdEn6rCv3 REdHn2v3, REdMn2rCv3, REdMn2v3, REeEn2tMv3, REeEn3p0rHv3, REeMn2tMv3
DQ-4	REdEn2rCv4, REdEn2rHv4, REdEn2rMv4, REdEn2v4, REdEn3rCv4, REdEn3rHv4, REdEn3rMv4, REdEn3v4, REdEn4rHv4, REeEn2rHv4

DQ-3 consists of 12 sub-datasets and DQ-4 consists of 10 sub-datasets, with their names listed in [Table 3](#). The rules for generating these sub-datasets are encoded in their names. For instance, the dataset REdEn4rCv3 consists of randomly generated systems in three variables (v3). The system has 4 constraints (n4) and each constraint in the system is a pure polynomial (rC) of total degree in the range of 1..2 (dE). The other settings, such as the number of terms and the value of coefficients take the default value (RE), specified in Table 1 of [Chen et al. \(2024\)](#). These raw datasets are preprocessed following the rules in [Section 4.4](#). The final sizes of the four datasets are summarized in

Table 4. To be specific, the training set is used for model training, the validation set is used to evaluate the model’s performance during the training process, the testing-validation set is used for model prediction evaluation after training completion, and the holdout testing set is used for the final evaluation (used only once and never seen before the final test) of the model.

Following the same protocol for generating the DQ-3 and DQ-4 sub-datasets, we randomly generated 200,000 unlabeled examples (i.e. polynomial systems) for each sub-dataset. These were then split into training, validation, testing-validation, and testing sets in a 7:1:1:1 ratio. The datasets are preprocessed following the steps described in Section 4.4. Furthermore, the preprocessing procedure is tailored to the specific features of each task. In `task_m`, polynomial systems with excessively long product sequences are pruned by retaining only those with a sequence length ≤ 512 . For `task_p` and `task_s`, a small number of degenerate cases with an empty projection factor set (pf) are discarded. Furthermore, in the four-variables scenario, a 3-second timeout per example is enforced during feature computation for `task_r` and `task_s` in Maple to ensure feasibility. Examples exceeding this limit are discarded. The final dataset sizes are presented in Table 4.

Table 4: Data size for each task.

Dataset	Task	Train	Valid	Test-Valid	Test
DQ-3	<code>task_c</code>	8,724	1,238	1,214	1,215
	<code>task_e/task_f/task_r</code>	1,680,000	240,000	240,000	240,000
	<code>task_m</code>	1,155,452	165,020	164,935	165,068
	<code>task_p/task_s</code>	1,679,997	240,000	239,999	239,999
DQ-4	<code>task_c</code>	10,574	1,488	1,180	1,180
	<code>task_e/task_f</code>	1,400,000	200,000	200,000	200,000
	<code>task_m</code>	1,168,113	166,865	166,772	167,034
	<code>task_p</code>	1,399,999	200,000	200,000	200,000
	<code>task_r</code>	1,399,998	200,000	200,000	200,000
	<code>task_s</code>	1,399,996	200,000	200,000	200,000

It is important to note that, due to practical considerations such as prolonged training time and the substantial computational cost associated with hyperparameter tuning, we do not directly employ the full pre-training datasets in the initial training and evaluation stages. Instead, using a fixed random seed, we randomly sample one-tenth of the data from each pre-training task to serve as the learning corpus. This strategy not only substantially reduces training time and experimental overhead but also enables more efficient exploration of model architectures and hyperparameter configurations within a manageable experimental scale, thereby laying a solid foundation for subsequent large-scale training on the complete datasets.

5.2. An enhanced 4-variable random dataset

In this section, we introduce an enhanced four-variables dataset, denoted as DQ-4b. This dataset is constructed by substantially augmenting the number of polynomial instances in the original DQ-4 dataset presented in Chen et al. (2024). As a result, DQ-4 is a strict subset of DQ-4b. More precisely, we expand the existing sub-dataset REeEn2rHv4 in DQ-4 and introduce two additional sub-datasets, REeEn3rHv4 and REcMeEn3p0rCv4. In addition, we generate pre-training data for these two new sub-datasets following the same procedure used for the other sub-datasets in DQ-4. The newly generated pre-training data are then combined with the existing DQ-4 pre-training data to form the full pre-training corpus for DQ-4b. Due to constraints on training time and computational resources, we randomly sample one-tenth of this full corpus for use in the DQ-4b pre-training tasks. Table 5 reports the amount of data used for each task. Finally, for consistency in task naming, we designate `task_b` as the identifier for the CAD variable-ordering selection task on the DQ-4b dataset.

Following the methodology described in Chen et al. (2024), for each system we compute the maximum CAD running time, denoted by `max`, over all 24 possible variable orderings. Each sub-dataset is then partitioned into five time intervals according to their corresponding `max` values, as shown in Figure 3. From the distribution, we observe that the expanded sub-dataset and the two newly added sub-datasets (corresponding to the three rightmost bars in

Table 5: Data size for tasks related to DQ-4b.

Task	Train	Valid	Test-Valid	Test
task_b	12,366	1,741	1,431	1,431
task_e/task_f/task_r	168,000	24,000	24,000	24,000
task_m	124,789	17,815	17,702	17,796
task_p	167,999	24,000	24,000	24,000
task_s	167,813	23,982	23,962	23,969

the figure) contain a substantially higher proportion of difficult instances—those with $\max \geq 100s$ —compared to the remaining sub-datasets.

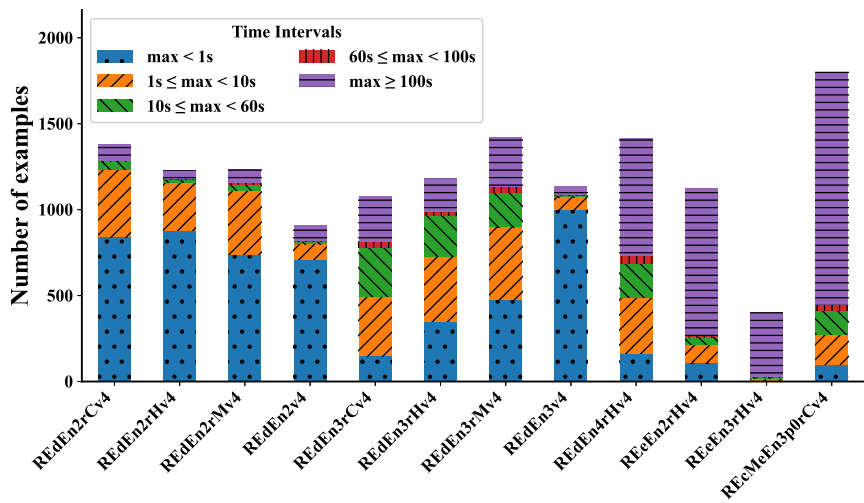


Figure 3: Distribution of the number of examples according to different ranges of \max for RE-Subsets in DQ-4b.

For a given system, let t_{\min} denote its minimum CAD running time under all variable orderings. Let O_{rel} be the set of all relative optimal orderings, that is the orderings whose corresponding CAD running times do not exceed $1.03 t_{\min}$. Let O be the set of all variable orderings, and define $\bar{O} := O \setminus O_{\text{rel}}$. Let $t_{\max_{O_{\text{rel}}}}$ (resp. $t_{\min_{\bar{O}}}$) be the maximum (resp. minimum) CAD running time under the orderings in O_{rel} (resp. \bar{O}). We define the *performance gap ratio* as $t_{\max_{O_{\text{rel}}}} / t_{\min_{\bar{O}}}$, which measures the performance advantage of the relative optimal orderings over the rest. Here smaller values indicate better data quality. The box plot in Figure 4 illustrates the distribution of this ratio across all DQ-4b sub-datasets. The third quartile (and median) values of the three rightmost sub-datasets are noticeably smaller than those of the others, indicating their superior quality.

5.3. SMT dataset

In this section, we briefly review a dataset relevant to SMT solving, which is called SMT CAD Order Data in this paper, introduced in [del Rio Almajan and England \(2022\)](#). This dataset consists of 1,019 instances, each comprising a set of polynomials in three variables. Its purpose in our study is to evaluate whether our model trained on randomly generated data can generalize effectively to practical SMT inputs. For this purpose, the SMT CAD Order Data is partitioned into training, validation, testing-validation, and testing splits using a 7:1:1:1 ratio. The training subset is used to fine-tune both the pre-trained model and the CAD-fine-tuned model. The experiments taken on this dataset are introduced in Section 7.2.3.

Figure 5 presents the distributions of these examples with respect to the number of constraints, the number of terms, the total degrees, and the density of coefficients. Figures 5a, 5b, and 5c show that most examples have 5–9

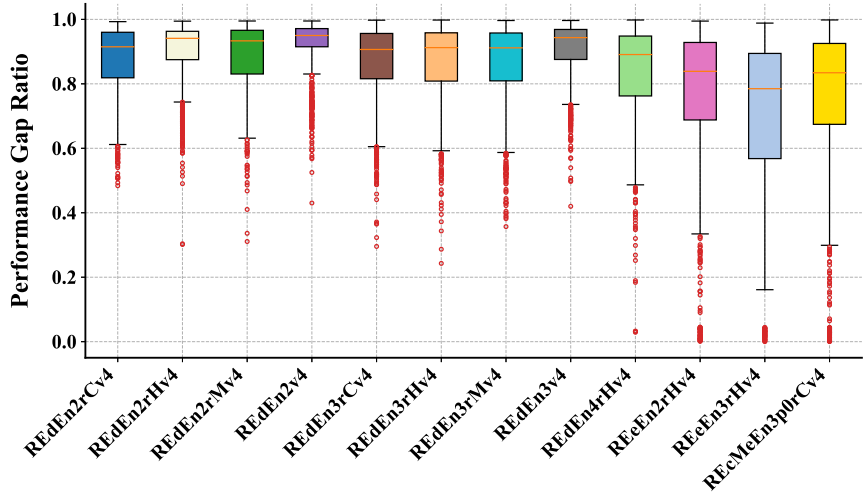


Figure 4: Performance gap ratios for RE-Subsets in DQ-4b.

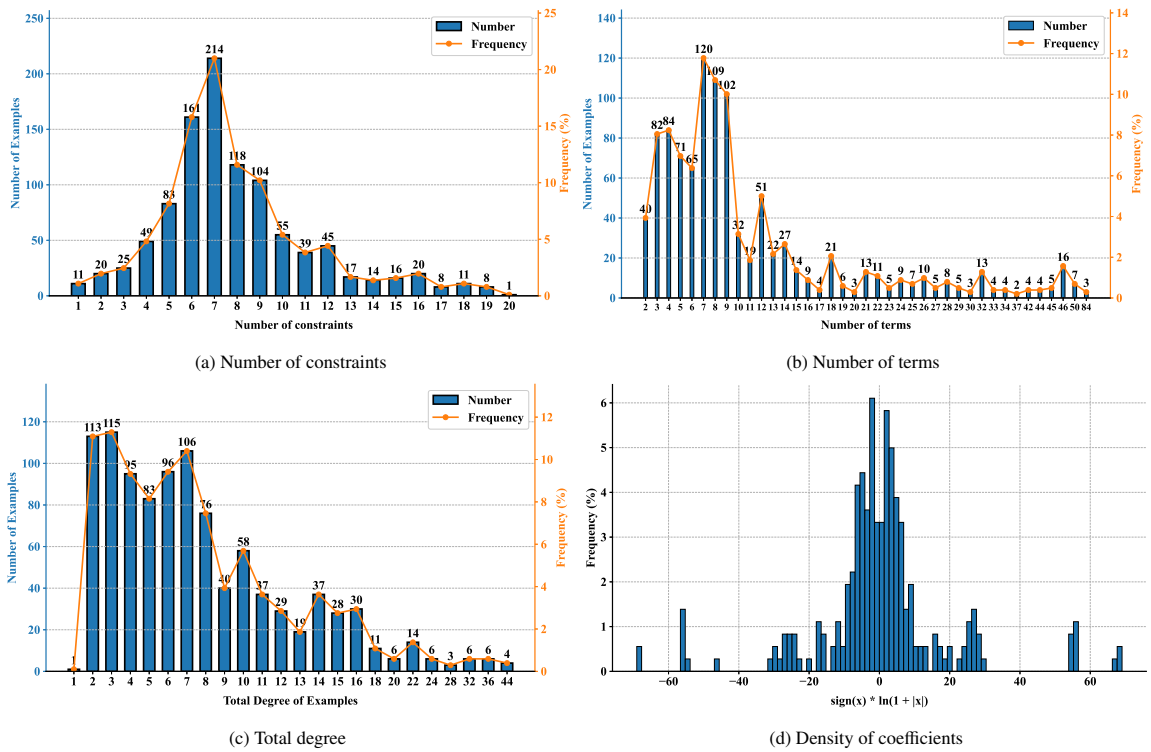


Figure 5: Statistical information of the SMT CAD order dataset.

constraints, 3–9 terms, and total degrees ranging from 2 to 8. For any system, we choose the maximum and the minimum of all its coefficients, and apply the logarithmic transformation, that is $x \rightarrow \text{sign}(x) \cdot \ln(1 + |x|)$. Figure 5d reports the distribution of these values across all systems in the dataset. It shows a clear central peak around 0, with the distribution tapering off symmetrically in both directions.

6. Heuristic baselines

To better evaluate the performance of Transformer models, in this section, we present 11 heuristic methods for CAD variable ordering selection as baselines and evaluate their performance on four CAD order datasets. Five of them are existing heuristics, including the classical Brown’s heuristic method `svob` Brown (2004), the command `SuggestVariableOrder` in the `RegularChains` library of Maple Chen et al. (2011) (`svoc` for short), and three recent ones: `gmods` in del Rio Almajan and England (2022), the pseudo graph feature `pgf` Chen et al. (2020), and `tone` (T1 in Pickering et al. (2024a)). The rest are variants of them.

6.1. Introduction of the heuristics

The heuristic methods for suggesting a variable ordering for CAD are based on sorting the feature vectors associated with the variables. More precisely, let $F \subset \mathbb{Q}[x_1, \dots, x_n]$. For each variable x_i , one computes a feature vector \mathbf{y}_i of a fixed size s and appends i to the end of \mathbf{y}_i to break the tie. One then sorts the vectors $\mathbf{y}_1, \dots, \mathbf{y}_n$ in the lexicographical ascending order into $\mathbf{y}_{i_1}, \dots, \mathbf{y}_{i_n}$. Then the corresponding suggested variable ordering is $x_{i_1} > \dots > x_{i_n}$.

Table 6: Heuristic methods for CAD.

Heuristic	Features
<code>svob</code>	(<code>max_max_d</code> , <code>max_max_e</code> , <code>sum_sum_a</code>)
<code>svoc</code>	(<code>max_max_d</code> , <code>max_l</code> , <code>sum_max_d</code>)
<code>gmods</code>	(<code>sum_max_d</code>)
<code>tone</code>	(<code>sum_max_d</code> , <code>avg_avg_d</code> , <code>sum_sum_d</code>)
<code>slm</code>	(<code>sum_max_d</code> , <code>max_l</code> , <code>max_max_d</code>)
<code>SmSsAa</code>	(<code>sum_max_d</code> , <code>sum_sum_d</code> , <code>avg_avg_d</code>)
<code>SmAaMI</code>	(<code>sum_max_d</code> , <code>avg_avg_d</code> , <code>max_l</code>)
<code>isf</code>	$ie_{11}(F)$
<code>psf</code>	$ie_{11}\left(\bigcup_{i=1}^n pf(F, x_i)\right)$
<code>ipf</code>	$(ie_{11}(F), ie_{11}\left(\bigcup_{i=1}^n pf(F, x_i)\right))$
<code>pgf</code>	pseudo graph feature vector of F

Different heuristic methods compute different feature vectors. Table 6 summarizes the state-of-the-art heuristic methods as well as their variants. In the table, given $F = \{f_1, \dots, f_m\}$ and a variable v , `max_l` is a number computed in the following way. For each f_i , let $d_i = 0$ if v does not appear in f_i , and otherwise let d_i be the total degree of the leading coefficient of f_i w.r.t. v . The number `max_l` is then assigned to be the maximum element of $\mathbf{l} := \{d_1, \dots, d_m\}$. It is interesting to observe that the quantities `d` and `a` are only relevant to a given variable v , while the quantifiers given by `e`, `l` as well as the pseudo graph feature vectors reveal also the impact of the rest variables on v . The top 8 heuristics and `pgf` listed in Table 6 rely only on explicit information from the input polynomials, and thus can be applied on the fly to select a variable ordering. The rest two heuristics involve the computation of resultants of input polynomials and thus may consume more time.

6.2. Evaluation of the heuristics

Based on the formal definitions of the heuristic methods introduced above, this section evaluates their performance on the CAD order datasets (i.e. SMT, DQ-3, DQ-4 and DQ-4b) presented in Section 5. Table 7 presents the absolute accuracy, the relative accuracy, and the time ratio for the heuristic methods evaluated on the four CAD datasets. The best value in each column is highlighted in bold. Here, for a given example, time ratio measures the ratio of the

Table 7: Performance comparison of heuristic methods across CAD datasets.

Heuristics	Abs_Acc (%)				Rel_Acc (%)				Time_Ratio			
	SMT	DQ-3	DQ-4	DQ-4b	SMT	DQ-3	DQ-4	DQ-4b	SMT	DQ-3	DQ-4	DQ-4b
svob	55.45	37.86	20.41	18.06	67.32	41.07	27.69	24.38	1.25	6.86	3.85	4.50
svoc	53.88	37.45	18.26	16.64	65.36	40.61	25.16	22.64	1.31	8.46	4.46	4.41
gmods	56.72	44.57	15.78	15.30	68.89	48.13	22.16	20.98	1.18	5.73	3.76	3.68
tone	54.17	46.96	18.92	17.54	66.44	50.66	26.05	23.82	1.18	5.36	3.61	3.87
s1m	55.64	46.20	18.35	17.45	67.91	49.81	25.27	23.60	1.18	5.65	3.84	3.69
SmSsAa	54.96	46.90	18.81	17.48	67.12	50.51	25.93	23.76	1.19	5.28	3.62	3.84
SmAaM1	54.27	47.75	20.31	18.66	66.63	51.40	27.89	25.30	1.18	5.37	3.57	3.86
isf	55.25	48.53	20.71	19.20	67.81	52.32	28.15	25.75	1.19	5.28	3.60	3.79
psf	40.63	29.94	22.15	21.04	50.74	32.55	29.78	28.04	1.55	7.65	4.23	3.41
ipf	55.05	48.51	21.51	19.86	67.71	52.35	29.24	26.63	1.20	5.28	3.60	3.78
pgf	53.58	47.75	19.44	18.13	66.05	51.38	26.48	24.38	1.33	5.51	3.68	3.75

running time of CAD for this example under the ordering selected by the heuristic over the minimal running time of CAD under all possible variable orderings. Note that for this evaluation, the entire data of each dataset is used.

From Table 7, we have the following observations. Among all four datasets, the SMT dataset is much less challenging than the others in terms of both accuracy and time ratio. On the SMT dataset, gmods outperforms the others in terms of both accuracy and time ratio. On DQ-3, isf and ipf perform the best. On DQ-4, psf and SmAaM1 outperform the others in terms of accuracy and time ratio respectively. On DQ-4b, psf outperforms the rest for both accuracy and time ratio. Overall, no heuristic methods dominate on all datasets.

Interestingly, only by reordering the features in svoc, the resulting heuristic s1m performs much better than svoc on all datasets. The top feature in s1m is now the same as in gmods and tone, that is sum_max_d. This feature reflects the partial degree of the product of input polynomials w.r.t. each variable, which plays an important role in measuring the complexity of CAD [del Rio Almajan and England \(2022\)](#). We remark that svoc was originally not designed as a dedicated variable ordering selection method for CAD. Rather it targeted on algorithms solving (mainly) polynomial equations based on triangular decompositions, which explains the appearance of the feature max_max_d (measuring maximum partial degree of the polynomials) and max_l (measuring total degree of the leading coefficient). The heuristic SmAaM1 replaces the last feature sum_sum_d in tone by the feature max_l. On all the datasets, it attains higher accuracy than tone. It also achieves the lowest time ratio on DQ-4.

From Table 7, we also observe that there is certain disagreement between the highest accuracy and the lowest time ratio. In particular, psf achieves the highest accuracy on DQ-4, but its time ratio is worse than most of the other heuristics. To further analyze this, we visualize the performance of all heuristics on all sub-datasets of DQ-4 and DQ-4b in Figure 6 (the first ten sub-datasets belong to DQ-4). From this figure, We notice that on the fifth sub-dataset REdEn3rCv4, psf achieves the highest accuracy but also the highest time ratio. On the contrast, although the accuracy of ipf is apparently lower than psf, it attains the lowest time ratio. To understand such a contradiction between accuracy and time ratio on the sub-dataset REdEn3rCv4, we further split REdEn3rCv4 into two subsets: *Normal_Set* and *Abnormal_Set*. The *Normal_Set* consists of examples where no timeout occurs for any variable ordering and the *Abnormal_Set* consists of the rest of examples. Table 8 compares the total CAD running time under the variable orderings predicted by psf and ipf on these two sub-datasets of different difficulty. From the table, we see that when psf makes a wrong prediction, it is penalized much more than ipf on the more difficult dataset *Abnormal_Set*.

7. Experiments

In this section, we present the experimental results. Experiments were performed on a workstation with an Intel Xeon Platinum 8272CL CPU @ 2.60 GHz, 256 GB RAM, and an NVIDIA RTX 4090 GPU, running Ubuntu 22.04. The software environment includes Python 3.10 and Maple 2024. The content is organized as follows. Firstly, we describe the architectures and hyperparameters selected after extensive tuning to achieve optimal performance on the

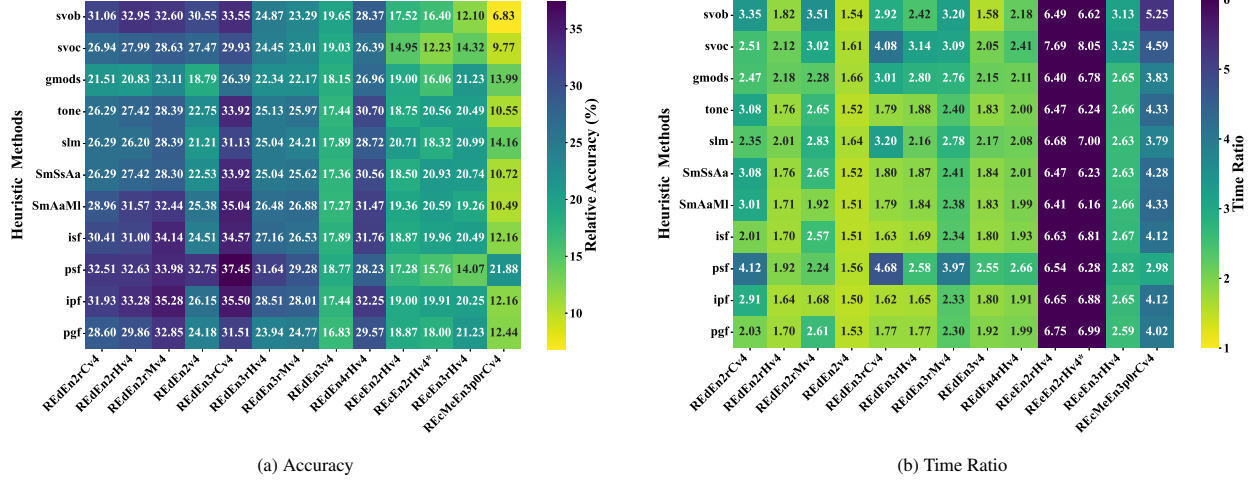


Figure 6: Performance of the heuristics on all sub-datasets of DQ-4 and DQ-4b.

Table 8: Further experiments on the dataset REdEn3rCv4.

Category (number)	Heuristic	n_time	ab_time	timeout
Both correctly predicted (236)	psf	42.08	19.55	0
	ipf	42.05	19.54	0
Both wrongly predicted (527)	psf	432.44	1429.94	1
	ipf	300.70	215.98	0
psf correct but ipf wrong (167)	psf	36.82	53.30	0
	ipf	91.76	76.44	0
psf wrong but ipf correct (146)	psf	97.61	300.90	0
	ipf	46.86	42.07	0

validation sets of `task_c`. We have also evaluated the performance of these models on the testing-validation dataset to have a feeling on the generalization ability of these models. Secondly, we report the performance of these models on hold-out testing datasets. We emphasize that the testing datasets were never seen by the tested models before the final test. By default, only the results on the testing datasets are shown. However, when there is an obvious performing difference between testing-validation and testing datasets, we present both experimental results to avoid the bias due to data splitting. Thirdly, we present several (including unsuccessful) attempts made aiming to push the limit of pre-training & fine-tuning for CAD variable ordering selection.

7.1. Detailed information on the architecture and parameters

In this study, all models are built upon a Transformer-based architecture. The architectural specifications and training configurations including batch size, optimizer settings (Adam with a fixed learning rate of 0.0001), dropout rate, and early stopping criteria are summarized in Table 9. The experimental workflow begins with a pre-training stage, where six models are trained, each corresponding to one of the six pre-training tasks. For fine-tuning, the pre-trained weights are used for initialization. The embedding layer and the first three encoder layers are frozen, while the remaining parameters are updated on the CAD order datasets. This procedure produces task-specific fine-tuned models optimized for CAD variable ordering prediction.

In addition, following the data processing strategy outlined in Section 5.1, we utilized the *HuggingFace Datasets library* [Lhoest et al. \(2021\)](#) for data loading and storage, adopting the Apache Parquet format [Vohra \(2016\)](#). This columnar storage format supports efficient compression and parallel processing, significantly improving data-loading

performance. Compared with plain text storage, it greatly accelerates data access and facilitates the efficient reuse of training data across multiple tasks, thereby enhancing the overall efficiency of the experimental workflow.

Table 9: Summary of model architecture and training parameters.

Category	Parameter	Value/Description
Model Architecture	Embedding Dimension	256
	Attention Heads	8
	Encoder Layers	7
	Decoder Layers	6
Training Configuration	Batch Size	128 (64 for <code>task_m</code> on 4-variable data)
	Epoch Definition	Each epoch spans the entire training set
Optimization	Optimizers	2 (independent: one for encoder, one for decoder)
	Optimizer Algorithm	Adam
	Learning Rate	0.0001 (fixed)
Regularization & Early Stopping	Dropout Rate	0.1
	Early Stopping Patience	30 consecutive epochs (no improvement in validation accuracy)
	Model Selection	Checkpoint with highest validation accuracy
Pre-training Strategy	Number of Pre-training Models	6 (one for each pre-training task)
Fine-tuning Strategy	Initialization	Pre-trained weights
	Frozen Layers	Input embedding layer + lowest 3 encoder layers
	Adapted Parameters	Remaining parameters
Data Handling	Dataset Storage Format	Parquet (for direct access and faster loading)
	Data Reuse	Cached data reused for tasks sharing identical training data

Remark 1. Table 9 presents the hyperparameter configuration employed for our main experiments. However, this specific parameter set was not arbitrarily chosen; rather, it is the culmination of extensive exploration and careful consideration. Indeed, prior to this, we conducted a substantial number of experimental explorations through systematic hyperparameter search and evaluation. Recognizing that a full training run for each hyperparameter combination would be computationally prohibitive and time-consuming, we adopted an efficient trial-training strategy: each hyperparameter trial was limited to the first 10 epochs, during which the validation set accuracy's evolution and performance were continuously monitored. This approach enabled us to effectively filter out underperforming parameter combinations within a significantly shorter timeframe. Following extensive trial-training and comparative analysis, evaluated mainly on the validation set of DQ-3, we ultimately determined the optimal hyperparameter set presented in Table 9.

7.2. Performance of the Transformer models

This section reports the performance of Transformer models on both the pre-training tasks and CAD variable ordering prediction tasks.

7.2.1. Performance on pre-training tasks

The performance of models for six pre-training tasks on three random datasets are reported in Table 10. Here, “valid”, “test-valid”, “test” refer to the validation set, the testing-validation, and the testing set, respectively. Note that, the performance on the validation set is obtained in the teacher-forcing mode while the performance on the testing-validation and testing sets are obtained in the autoregressive mode. The data on the same task show that inference in autoregressive mode does not lead to performance degradation. In addition, the similarity between the performance on validation, test-validation and testing sets shows that the models have good in-distribution generalization ability.

Now, we focus on the performance of these models on the test data. For the two simple tasks (`task_e` and `task_f`) only involving extracting the features of input systems, the pre-training models achieve nearly perfect accuracies. For the slightly more complex polynomial multiplication task (only predicting supports of the product), the accuracies are all higher than 90%. The accuracies drop dramatically for those much more complex pre-training tasks, which involve the computation of resultants. For these more complex tasks, it is interesting to observe that the pre-training models perform better on four-variables datasets than the three-variables dataset. To understand the performance difference for different tasks on different datasets, we introduce the **mean feature-digit length** to measure the difficulty of the output. More precisely, recall that the output of every example for each pre-training task consists of a set m of features

Table 10: Accuracies of pre-training tasks.

Dataset	Category	task_e	task_f	task_m	task_p	task_r	task_s
DQ-3	valid	100.00%	98.00%	93.49%	25.29%	20.28%	9.30%
	test-valid	99.99%	98.08%	93.65%	24.75%	19.93%	9.22%
	test	100.00%	98.11%	93.78%	24.87%	19.83%	9.02%
DQ-4	valid	99.99%	99.83%	94.03%	65.88%	49.80%	41.01%
	test-valid	99.98%	99.85%	93.91%	65.49%	49.44%	41.24%
	test	100.00%	99.79%	94.25%	65.14%	49.36%	40.76%
DQ-4b	valid	99.98%	99.90%	93.08%	56.62%	41.57%	35.19%
	test-valid	99.98%	99.90%	92.75%	56.02%	41.31%	35.46%
	test	100.00%	99.99%	93.32%	56.09%	41.03%	35.10%

and each feature is a n -tuple of integers, where n is the number of variables. The mean feature-digit length is defined as the total number of digits across all feature values divided by mn . For every pre-training task, we then average this quantity across all instances in the corresponding test set, yielding the mean feature-digit length summarized in Table 11. By comparing the values in this table with the accuracies of three tasks reported in Table 10, we see that the mean feature-digit length does characterize the learning difficulty of the three tasks across the testing set.

Table 11: Comparison of the mean digit length for each pre-training task on testing set.

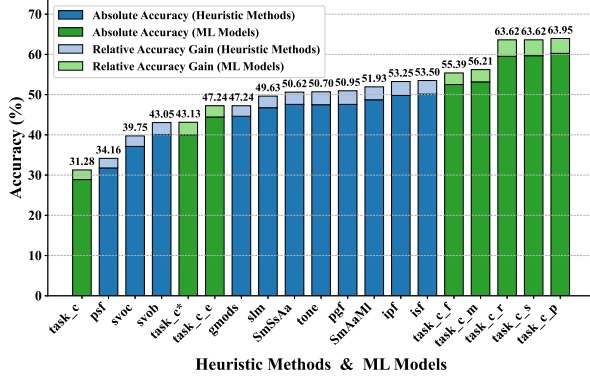
Data	task_p	task_r	task_s	Data	task_p	task_r	task_s	Data	task_p	task_r	task_s
DQ-3	1.83	2.12	2.75	DQ-4	1.34	1.60	2.20	DQ-4b	1.48	1.79	2.46

7.2.2. Performance for CAD variable ordering selection on three random datasets

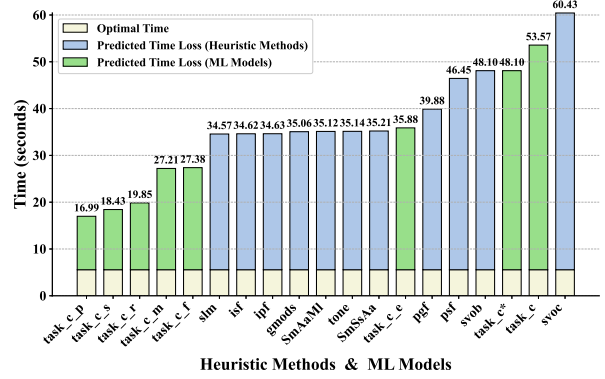
Figure 7 compares the performance of ML models and heuristic methods for CAD variable ordering selection in terms of both (relative) accuracy and CAD running time on the three variable random dataset DQ-3. In the figure, the ML models start with the word “task”. We have the following observations: (i) The pre-training & fine-tuning models involve “CAD projection” (task_c_p, task_c_s, task_c_r), thus learning deep features, achieve the highest accuracy and the lowest CAD running time. Running CAD under the variable ordering selected by the best pre-training model achieves more than **2 \times speedup** over running CAD under the one selected by the best heuristic method; (ii) The pre-training & fine-tuning models involve “light computation” (task_c_m, task_c_f), learning shallow features of the input system, also outperform the best heuristic, although less promising than those involving “CAD projection”; (iii) Direct Transformer models (task_c, task_c^{*}) underperform most of the heuristics, which further justify the importance of pre-training and fine-tuning; (iv) The naive pre-training model task_c_e, predicting only the exponent vectors of input system, still performs better than direct Transformer models, although underperforms most of the heuristics.

In Figure 7, the only difference between task_c^{*} and task_c is that they use different tokenization schemes. The latter used the default scheme introduced in Section 4.5 while the former used the alternative scheme detailed in Section 7.3.5. As shown in Figure 7, for direct Transformer models, the former scheme performs better. However, the tokenization scheme has different impacts on different tasks. A comprehensive evaluation is provided in Section 7.3.5.

Figure 8 compares the performance of ML models with heuristic methods on testing and testing-valid set of the random four variables dataset DQ-4. The performance of some of the models on these two sets are different. So we include both in order to draw a more solid conclusion. Firstly, for both figures, the trend observed in (i) for DQ-3 still holds here. The three pre-training models learning deep features still perform the best after fine-tuning, although the speedup over the best heuristic is less significant (**1.3 \times** on testing set). Secondly, the pre-training model task_c_f learning the shallow features still outperforms most of the heuristics as well as the direct Transformer models after fine-tuning. The other pre-training model task_c_m, however, does not perform as well as in the three variable case.

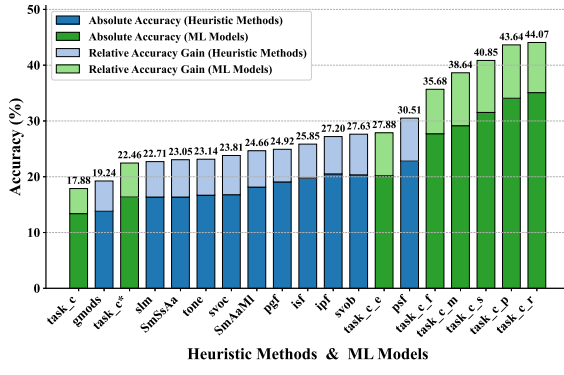


(a) Accuracy results.

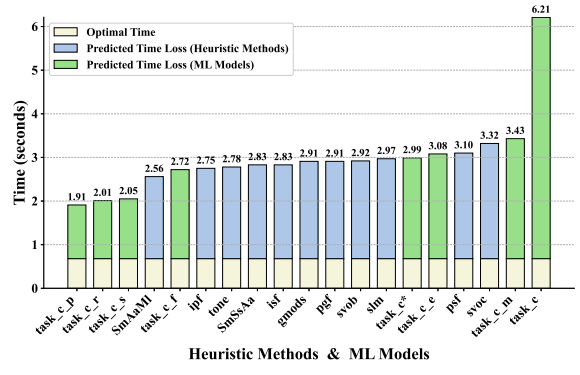


(b) Execution time results.

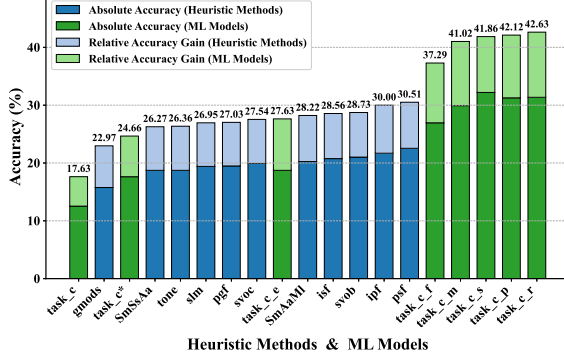
Figure 7: Comparison of heuristic methods and ML models on the DQ-3 testing set.



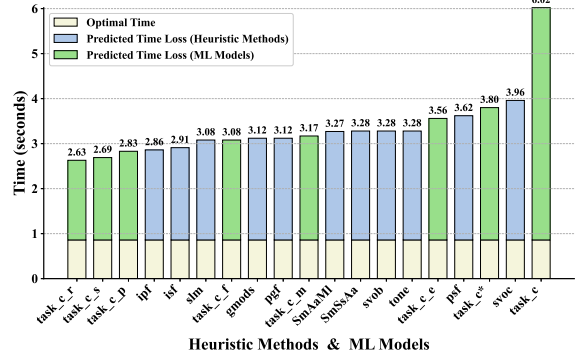
(a) Accuracy results on the testing-set.



(b) Execution time results on the testing-set.



(c) Accuracy results on the testing-validation set.



(d) Execution time results on the testing-validation set.

Figure 8: Comparison of heuristic methods and ML models on the DQ-4 testing set and testing-validation set.

Next, we report the performance on DQ-4b, which includes DQ-4 as a subset and enhances DQ-4 with more difficult examples. The results are shown in Figure 9. All four observations (i) – (iv) made for DQ-3 apply here as well, except that the speedup of the best pre-training & fine-tuning model over the best heuristic is less significant (**1.4x** on testing set). We notice that, the speedup over the classical heuristic method `svob` is close to **2x**.

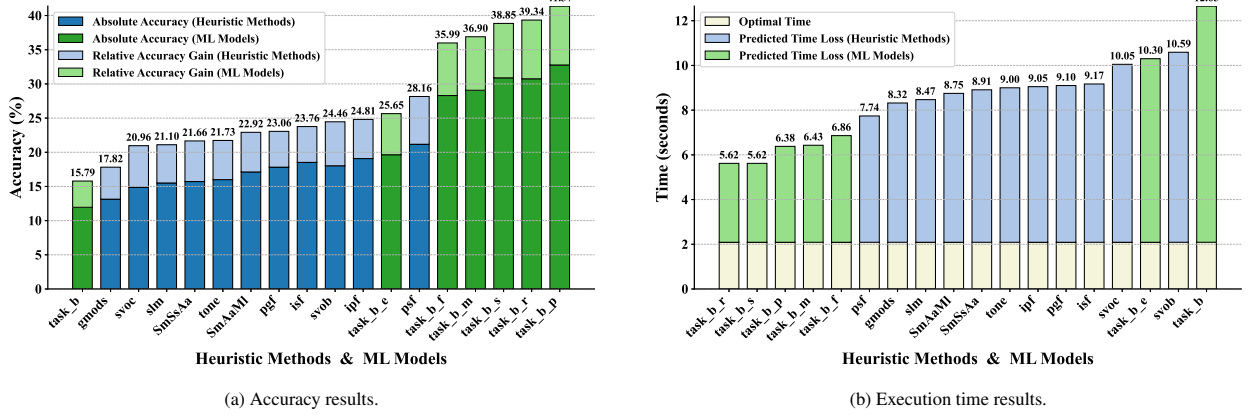


Figure 9: Comparison of heuristic methods and ML models on the DQ-4b testing set.

7.2.3. Performance on the SMT dataset

In this section, we present the performance of various models on the SMT dataset. The models under consideration are categorized into two groups : “Random Models” and “SMT Models”, illustrated in Figure 10:

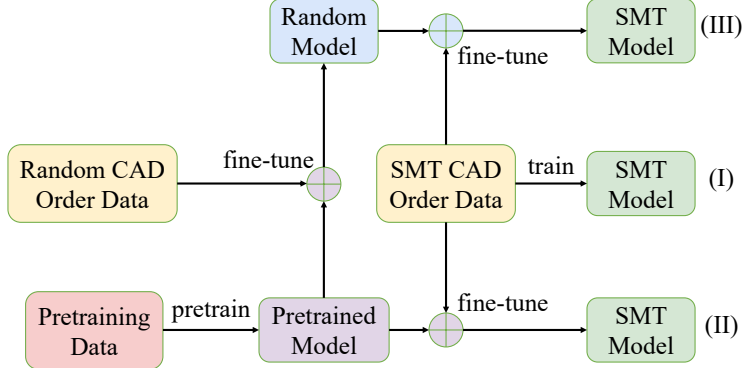


Figure 10: An overview of comparison for CAD model and SMT model.

- (1) **Random Models** These are the models that we have tested on the DQ-3 dataset. That is, they are either the Transformer models directly trained on DQ-3 or pre-trained model but fine-tuned on DQ-3. These models are not fine-tuned on the SMT dataset.
- (2) **SMT Models** The models in this category are further divided into three subcategories. The model in the first subcategory is obtained by directly training the Transformer model with the training set of the SMT dataset, denoted by `task_t`. The models in the second subcategory are obtained by directly fine-tuning those pre-trained models on the training set of the SMT dataset, named as `task_t_e`, `task_t_f`, `task_t_m`, `task_t_p`, `task_t_r`, and `task_t_s`. The models in the third subcategory are obtained by further fine-tuning those pre-trained models, which have already been fine-tuned on the CAD order dataset DQ-3, on the the training

set of the SMT dataset, named as `task_t_c_e`, `task_t_c_f`, `task_t_c_m`, `task_t_c_p`, `task_t_c_r`, and `task_t_c_s`.

Comparisons of 13 SMT models, 7 random models, and 11 heuristic methods are provided in Figures 11 and 12, measuring respectively the accuracy and CAD running time. We have the following observations: (i) The pre-trained models fine-tuned further on the SMT dataset perform the best. Most of these models (actually all pre-trained model exploiting deep features) outperform the best heuristic method; (ii) If the models are finally fine-tuned with the SMT dataset, then firstly fine-tuning on the random CAD order set does not help much and sometimes even reduce the performance; (iii) The pre-trained models not fine-tuned on the SMT dataset show limited generalization ability and they underperform most of the heuristic methods and the Transform model directly trained on the SMT dataset, although still outperform the one directly trained on the random dataset DQ-3.

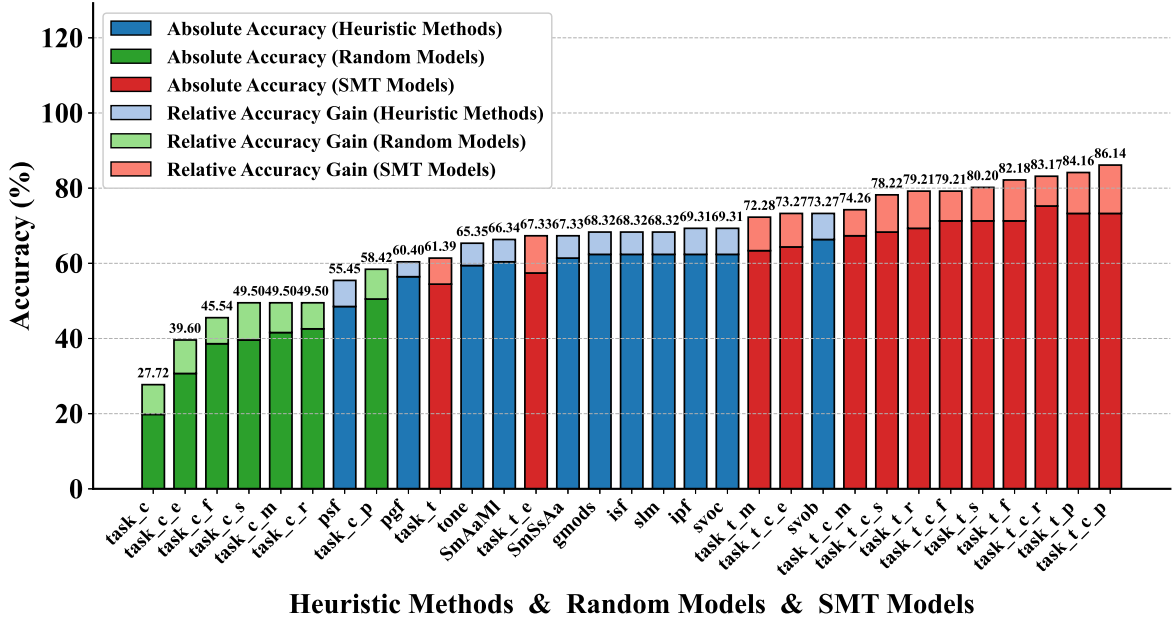


Figure 11: Accuracy comparison of heuristic methods and ML models on SMT testing-validation dataset.

7.3. Some attempts to push the limit of pre-training & fine-tuning models

From the evaluations on both random and real datasets in last subsection, we have the following common observations: (i) Pre-training & fine-tuning can substantially improve the performance of Transformer models on the CAD variable ordering selection task though firstly learning to predict some features relevant to the projection computation of CAD; (ii) Pre-training & fine-tuning brings such an improvement by creating labelled pre-training datasets 10 \times larger, but with much lower cost, than the variable ordering dataset.

These positive results encouraged us to explore in different directions aiming to further improve the performance. More precisely, this section is designed to further address the following research questions:

- (RQ₁) Can further performance improvement be achieved if the size of the pre-training dataset increases by another magnitude?
- (RQ₂) Can further performance improvement be achieved if we increase the capacity of Transformer models?
- (RQ₃) Instead of relying on pre-training to learn important features for CAD variable ordering selection, what if we first compute these features and directly use these features to train Transformer models?

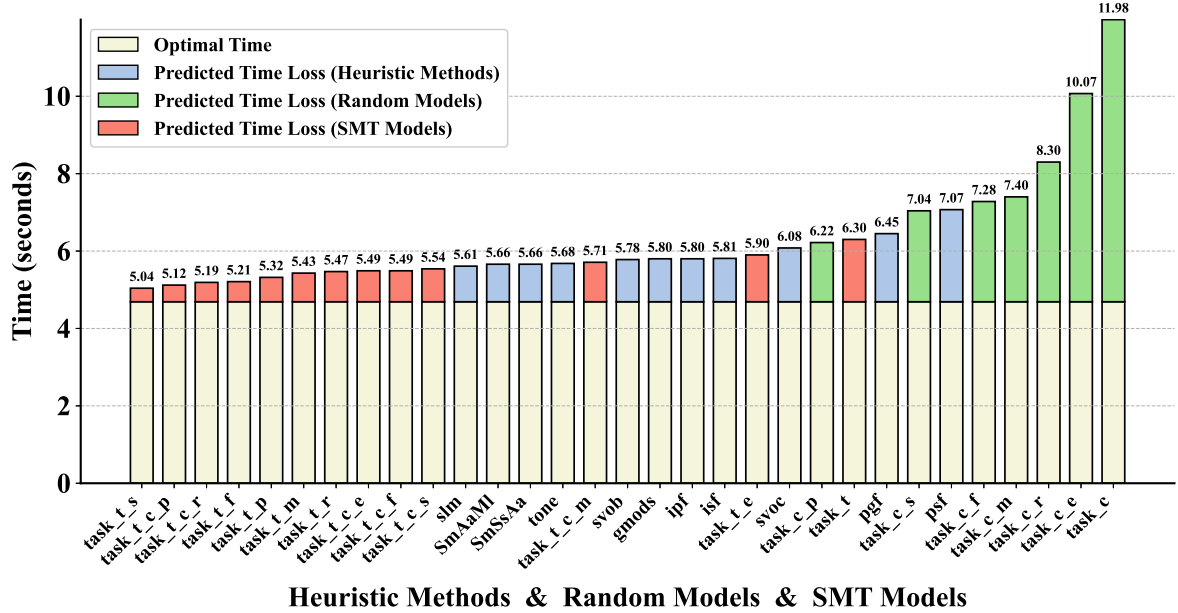


Figure 12: Runtime comparison of heuristic methods and ML models on SMT testing-validation dataset.

- **(RQ4)** As the performance of pre-training models is critical to the CAD order task, can we adopt a multi-stage pre-training scheme to further lift the performance?
- **(RQ5)** What is the impact of different tokenization schemes?

The evaluations for addressing these questions were made on the testing-validation sets of DQ-3.

7.3.1. The impact of dataset size on pre-training tasks and CAD order tasks

In Section 5.1, we successfully generated pre-training datasets comprising millions of instances for DQ-3. In the experimental results reported in Section 7.2, however, we only used 1/10 of the pre-training data for training the models. It is natural to ask what if all the pre-training data are used.

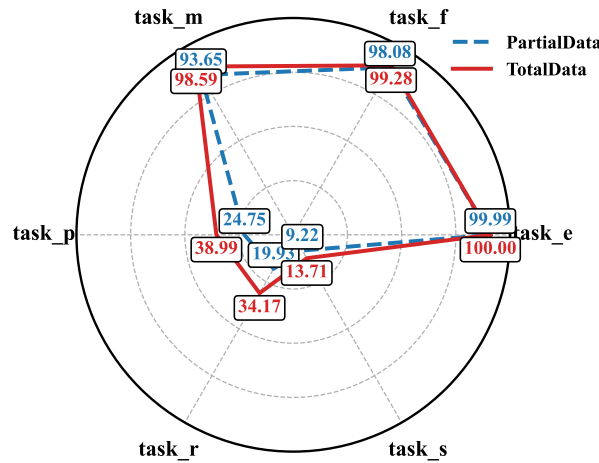


Figure 13: Performance comparison of pre-trained models with partial data and total data.

The impact of data augmentation strategies on the accuracy of pre-training models for three-variables and four-variables problems is illustrated in Figure 13. This chart compares the accuracies of six pre-training tasks under partial-data and total-data settings. On one hand, more data do boost the performance of models on difficult pre-training tasks, namely `task_p`, `task_r` and `task_s`. On the other hand, in the best case, the accuracy does not double even the size of the dataset gets 10x larger.

Still, given the previous experimental results revealing that limited accuracy on pre-training task greatly improve the performance on CAD ordering selection task, we expect that the pre-trained models trained with much more data can further lift such a performance. The experimental results are reported in Figure 14. Regarding the accuracy, the difference between the total-data and partial-data models are negligible on most of the tasks. For CAD running time, the total-data model slightly outperforms the partial-data model on four tasks but underperforms the total-data model on two tasks. As an answer to (RQ₁), overall, the benefit of further increasing the dataset size of pre-training datasets for pre-training tasks is significant, but the benefit of transferring to CAD order task is negligible.

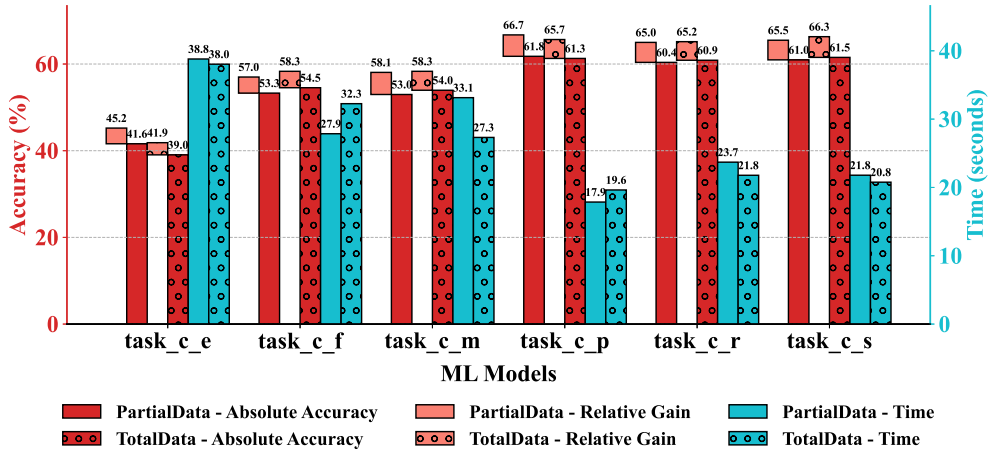


Figure 14: Performance comparison of models pre-trained with partial data and total data after fine-tuning on CAD order task.

7.3.2. The impact of model's capacity on pre-training tasks and CAD order tasks

In this section, we use `task_s` as an example to understand the impact of model's capacity on the performance. In Section 7.3.1, we have observed that increasing the dataset size can substantially improve the performance of pre-training models. As the dataset size has increased, it is natural to increase the model's capacity accordingly. Table 12 shows the changes. Note that limited to the hardware limit of our GPU, the batch size is reduced. We also reduce the number of encoders by one, but double the number of decoders. This adjustment is based on the observation from our previous experimental results, namely the accuracies of models on tasks for learning input features (namely `task_e` and `task_f`) are nearly perfect, but the accuracies of models on generating deep features for CAD ordering are relatively low. Thus, we slightly reduce the number of encoders, but significantly increase the number of decoders.

Table 12: Comparison on model architecture and training parameters.

Task_id	Embedding Dimension	Heads	Encoders/Decoders	Batch Size	Epochs
<code>task_s</code>	256	8	7/6	128	100
<code>task_ss</code>	512	16	6/12	32	100

For clarity and distinction, we designate the version of `task_s` trained with the new set of hyperparameters as `task_ss`. As shown in Table 13, the pre-training accuracy of `task_ss` significantly improved from **13.71%** for `task_s` to **18.57%**. This result strongly suggests that even for a challenging task like `task_s`, increasing the model's architectural capacity (through higher embedding dimensions, more attention heads, and deeper layers) leads to a

substantial improvement in pre-training performance. However, when transferred to CAD tasks, `task_ss` did not benefit from the more complex model architecture and enhanced hyperparameters. This provides an answer to (RQ₂).

Table 13: Performance variation after increasing the capacity of a pre-training model.

Pre-training Task	Accuracy	CAD Task	Abs_Acc	Rel_Acc	Predict_Time	Optimal_Time
<code>task_s</code>	13.71%	<code>task_c_s</code>	61.53%	66.31%	20.77	6.28
<code>task_ss</code>	18.57%	<code>task_c_ss</code>	61.29%	65.65%	22.02	6.28

7.3.3. Employing pre-training to learn features versus directly using features

In Section 4.3, we elaborated on the design of polynomial system pre-training tasks, where the core idea involves taking raw polynomial systems as input and generating a set of carefully designed, representative polynomial system features as output. Given the objective of generating these features, a natural and critical question arises: Do these features, extracted from the pre-training tasks, possess sufficient discriminative power to be directly applied to the CAD variable ordering task? More specifically, can we forgo the original polynomial system and instead use these features as direct model inputs, training a dedicated model with the CAD optimal ordering of the polynomial system as the target output?

To address this, for each pre-training task `task_x` presented in Table 1 of Section 4.3, we name its targeted learning object as `exp_x`. we compare two types of models: **RandomModel** and **FeatureModel**. The former model is the previously introduced pre-training & fine-tuning model, namely a model is trained to learn `exp_x` and then gets fine-tuned to learning the best CAD variable ordering. In contrast, the latter model is trained to predict the best variable ordering by taking directly `exp_x` as input.

A systematic comparison between RandomModel and FeatureModel across six pre-training tasks is presented in Figure 15. Overall, RandomModel consistently outperforms FeatureModel in the majority of tasks. The only exception occurs in `task_e`: FeatureModel attains slightly higher accuracy. But even in this case, FeatureModel does not show superiority on CAD running time. This provides an answer to (RQ₃): directly using pre-training derived features as model inputs is not optimal for downstream performance. Instead, employing such features as auxiliary tools during pre-training, facilitating knowledge transfer and representation learning, proves more effective. In this way, features help capture deep structures and latent distributional patterns, providing a robust initialization for subsequent adaptation.

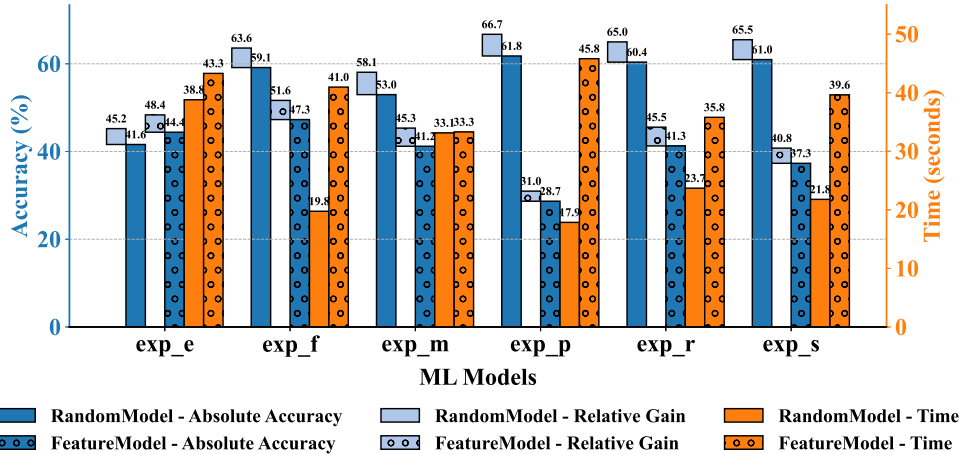


Figure 15: Performance comparison of RandomModel and FeatureModel on CAD order task.

7.3.4. The impact of multi-level pre-training

In Section 4.3, we designed several pre-training tasks aimed at effectively extracting features of polynomial systems and applying them to the CAD ordering task to enhance model performance. Building upon this, a natural question arises: if an individual pre-training task can successfully transfer to the CAD ordering task and improve model performance, could multiple sequential transfers between different pre-training tasks further boost the models capability by integrating and leveraging a broader range of pre-trained features?

To answer this question, we conducted a series of experiments. Here, we only show a representative example. As we know, `task_f` is designed to extract 11 core features of the input polynomials, whereas `task_p` focuses on capturing 11 key features related to the projection factor sets of input polynomials. In principle, the features learned in `task_f` should provide valuable assistance during the training process of `task_p`. Therefore, we first transferred the model pre-trained on `task_f` to the training phase of `task_p`. This sequential transfer task is denoted as `task_p_f`, whose main objective is to enhance the models learning capability for `task_p`. Subsequently, the model trained on `task_p_f` was further applied to the CAD ordering task, designated as `task_c_p_f`. Table 14 compares the performance between them. As shown in the results, the multi-transfer models did not outperform the single-transfer models. This provides an answer to (RQ4).

Table 14: Comparison of one-step and multi-step pre-training models.

Pre-training Task	Accuracy	CAD Task	Abs_Acc	Rel_Acc	Predict_Time	Optimal_Time
<code>task_p</code>	24.75%	<code>task_c_p</code>	61.78%	66.72%	17.86	6.28
<code>task_p_f</code>	22.48%	<code>task_c_p_f</code>	59.14%	63.59%	19.76	6.28

We attribute this performance degradation to the nature of the sequential transfer process. In multi-transfer settings, the final pre-trained model inherits the lower-level parameters from a simpler pre-training task, in this case, from `task_f`. Due to the fine-tuning strategy that freezes part of the models lower layers, the resulting representation space is dominated by features learned from the simpler task. However, such features are less effective for fine-tuning on complex downstream tasks, leading to suboptimal performance compared to models pre-trained directly on more complex tasks.

Moreover, it is important to note that the pre-training & fine-tuning paradigm is primarily designed for scenarios where labeled data for the target task is scarce. In such cases, pre-training on related labeled tasks can provide valuable prior knowledge for transfer. However, in our experimental setup, all pre-training tasks already contain sufficient labeled data, allowing the model to learn directly from large-scale supervision without requiring additional transfer steps. Consequently, performing multiple sequential transfers in this context does not yield further benefits and may even hinder the learning of task-specific representations.

7.3.5. The impact of tokenization

This section is designed to answer (RQ5). In Section 4.5, we have introduced a tokenization scheme for polynomials, hereafter referred to as Method-A, which completes omitted exponents (0 and 1) in polynomial expressions and distinguishes digits in coefficients and exponents w.r.t. the straightforward scheme proposed in Chen et al. (2024). However, we have already observed that Method-A underperforms the straightforward one for `task_c`. A preliminary investigation shows that if we only distinguish digits in coefficients and exponents but do not complete missing exponents w.r.t. the straightforward scheme, the resulting method, hereafter referred to as Method-B, outperforms both Method-A and the straightforward one for `task_c`. It is thus worth further investigating the impact of both Method-A and Method-B on the performance of other tasks. To illustrate Method-B, we consider the polynomial system discussed in 2. The encoding result produced by Method-A has already been presented in Section 4.5, while the corresponding result under Method-B is given as $\{\langle s \rangle, -, c6, *, x1, \wedge, 3, *, x2, -, c4, *, x1, *, x2, *, x3, \wedge, 2, +, c2, *, x2, \wedge, 2, *, x3, +, c1, =, c0, , -, c5, *, x3, \wedge, 4, +, x3, \wedge, 3, -, c7, =, c0, \langle /s \rangle\}$.

Figure 16 compares the performance of Method-A and Method-B on six pre-training tasks. We observe that Method-A (resp. Method-B) has a slight advantage over Method-B (resp. Method-A) on `task_p` and `task_r` (resp. `task_s`). Figure 17 further compares the performance of the two encoding schemes on pre-training & fine-tuning tasks for CAD variable ordering selection. On the best-performed tasks for ordering selection, the difference between the two is not significant. Method-A has a slight advantage over Method-B.

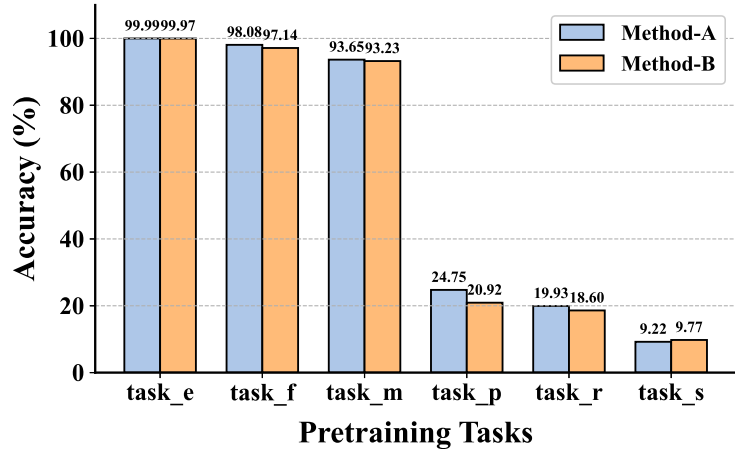


Figure 16: Comparison of two different tokenization schemes on pre-training tasks.

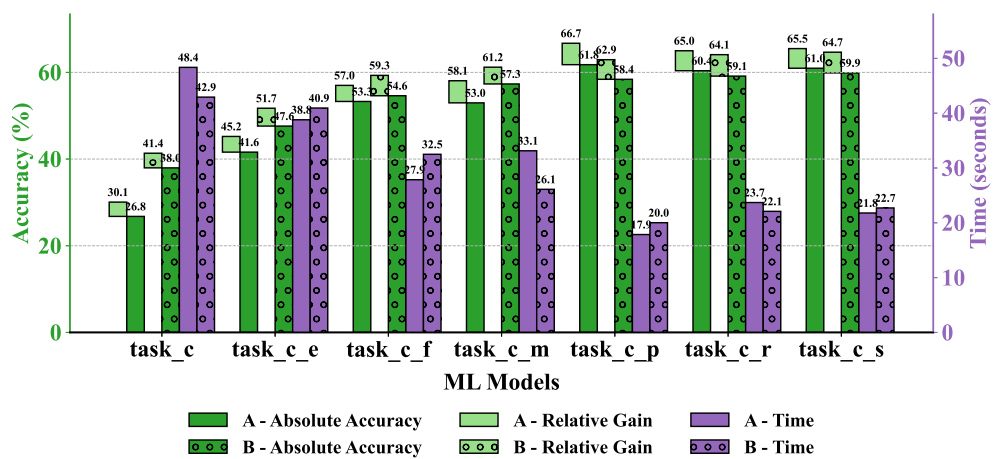


Figure 17: Performance comparison of Method-A and Method-B on seven transferred tasks under the CAD setting.

8. Conclusion and future Work

In this work, we proposed to leverage pre-training & fine-tuning Transformer models to address the inherent data scarcity problem when employing deep learning to predict the best variable ordering for cylindrical algebraic decomposition. By conducting intensive experiments on two publicly available random datasets, an enhanced random dataset and a real SMT dataset, we have demonstrated that the proposed approach substantially outperforms the state-of-the-art heuristic methods as well as Transformer models not employing the pre-training technique. On the dataset DQ-3, the best pre-training & fine-tuning model brings 2 \times speedup for CAD over the best heuristic approach, 3 \times speedup over the classical Brown's approach svob. On the dataset DQ-4b, the speedup over svob is near 2 \times . On a real SMT dataset, the model brings near-optimal performance (only 1.07 \times the optimal CAD running time).

We have also explored several different directions, such as increasing the pre-training dataset size and increasing the model capacity, aiming to push the limit of current work. We notice that, although the pre-training models have greatly helped the downstream CAD variable ordering selection task, the pre-training models for learning information of resultants still have a relatively low accuracy. For the future, much work remain to be done for learning with these basic symbolic operations, whose success may help with learning more advanced symbolic algorithms via the pre-training & fine-tuning paradigm.

Acknowledgements

The authors would like to thank Jürgen Gerhard for helping us getting Maple licence.

References

Alfarano, A., Charton, F., Hayat, A., 2024. Global lyapunov functions: a long-standing open problem in mathematics, with symbolic transformers. *Advances in Neural Information Processing Systems* 37, 93643–93670.

Barbosa, H., Barrett, C., Brain, M., Kremer, G., Lachnitt, H., Mann, M., Mohamed, A., Mohamed, M., Niemetz, A., Nötzli, A., et al., 2022. cvc5: A versatile and industrial-strength SMT solver, in: *International Conference on Tools and Algorithms for the Construction and Analysis of Systems*, Springer. pp. 415–442.

Bradford, R.J., Davenport, J.H., England, M., McCallum, S., Wilson, D.J., 2016. Truth table invariant cylindrical algebraic decomposition. *Journal of Symbolic Computation* 76, 1–35.

Brown, C., 2004. Tutorial: Cylindrical algebraic decomposition, at ISSAC.

Brown, C.W., 2001. Improved projection for cylindrical algebraic decomposition. *Journal of Symbolic Computation* 32, 447–465.

Brown, C.W., 2003. QEPCAD B: A program for computing with semi-algebraic sets using CADs. *ACM SIGSAM Bulletin* 37, 97–108.

Brown, C.W., Davenport, J.H., 2007. The complexity of quantifier elimination and cylindrical algebraic decomposition, in: *Proceedings of the 2007 International Symposium on Symbolic and Algebraic Computation*, Association for Computing Machinery, New York, NY, USA. pp. 54–60.

Brown, C.W., Košta, M., 2015. Constructing a single cell in cylindrical algebraic decomposition. *Journal of Symbolic Computation* 70, 14–48.

Chen, C., Davenport, J.H., Lemaire, F., Moreno Maza, M., Xia, B., Xiao, R., Xie, Y., 2011. Computing the real solutions of polynomial systems with the RegularChains library in maple. *ACM Communications in Computer Algebra* 45, 166–168.

Chen, C., Jing, R., Qian, C., Yuan, Y., Zhao, Y., 2024. A dataset for suggesting variable orderings for cylindrical algebraic decompositions, in: *International Workshop on Computer Algebra in Scientific Computing*, Cham: Springer Nature Switzerland. pp. 100–119.

Chen, C., Moreno Maza, M., 2014a. Cylindrical algebraic decomposition in the RegularChains library, in: International Congress on Mathematical Software, Springer Berlin Heidelberg. pp. 425–433.

Chen, C., Moreno Maza, M., 2014b. An incremental algorithm for computing cylindrical algebraic decompositions, in: Computer Mathematics: 9th Asian Symposium (ASCM2009), Fukuoka, December 2009, 10th Asian Symposium (ASCM2012), Beijing, October 2012, Contributed Papers and Invited Talks. Springer Berlin Heidelberg, pp. 199–221.

Chen, C., Moreno Maza, M., 2014c. Real quantifier elimination in the RegularChains library, in: Proceedings of International Congress on Mathematical Software, Springer Berlin Heidelberg. pp. 283–290.

Chen, C., Moreno Maza, M., Xia, B., Yang, L., 2009. Computing cylindrical algebraic decomposition via triangular decomposition, in: Proc. of ISSAC, ACM. pp. 95–102.

Chen, C., Zhu, Z., Chi, H., 2020. Variable ordering selection for cylindrical algebraic decomposition with artificial neural networks, in: roceedings of International Congress on Mathematical Software, Springer. pp. 281–291.

Chen, R., 2025. A geometric approach to cylindrical algebraic decomposition. *Mathematics of Computation* .

Collins, G.E., 1975. Quantifier elimination for real closed fields by cylindrical algebraic decomposition, in: Lecture Notes in Computer Science, Springer. p. 134183.

Collins, G.E., Hong, H., 1991. Partial cylindrical algebraic decomposition for quantifier elimination. *Journal of Symbolic Computation* 12, 299–328.

Corzilius, F., Kremer, G., Junges, S., Schupp, S., Ábrahám, E., 2015. SMT-RAT: An open source c++ toolbox for strategic and parallel SMT solving, in: International conference on theory and applications of satisfiability testing, Springer International Publishing, Cham. pp. 360–368.

del Rio Almajan, England, M., 2022. New heuristic to choose a cylindrical algebraic decomposition variable ordering motivated by complexity analysis, in: Proc. of CASC, Springer. pp. 300–317.

del Río Almajan, T., England, M., 2023. Data augmentation for mathematical objects, in: Proceedings of the 8th SC-Square Workshop, CEUR-WS.org. pp. 29–38.

Devlin, J., Chang, M.W., Lee, K., Toutanova, K., 2019. BERT: Pre-training of deep bidirectional transformers for language understanding, in: Proceedings of the 2019 Conference of the North American Chapter of the Association for Computational Linguistics: Human Language Technologies, Volume 1 (Long and Short Papers), Association for Computational Linguistics, Minneapolis, Minnesota. pp. 4171–4186.

Dolzmann, A., Seidl, A., Sturm, T., 2004. Efficient projection orders for CAD, in: Symbolic and Algebraic Computation, International Symposium ISSAC 2004, Santander, Spain, July 4-7, 2004, Proceedings, ACM. pp. 111–118.

Dutertre, B., 2014. Yices 2.2, in: International Conference on Computer Aided Verification, Cham: Springer International Publishing. pp. 737–744.

England, M., Florescu, D., 2019. Comparing machine learning models to choose the variable ordering for cylindrical algebraic decomposition, in: Intelligent Computer Mathematics - 12th International Conference, CICM 2019, Prague, Czech Republic, July 8-12, 2019, Proceedings, Springer. pp. 93–108.

Hester, J., Hitaj, B., Passmore, G., Owre, S., Shankar, N., Yeh, E., 2023. An augmented MetiTarski dataset for real quantifier elimination using machine learning, in: Intelligent Computer Mathematics, Springer Nature Switzerland, Cham. pp. 297–302.

Hong, H., 1990. An improvement of the projection operator in cylindrical algebraic decomposition, in: Proc. of ISSAC, pp. 261–264.

Huang, Z., England, M., Wilson, D., Davenport, J.H., Paulson, L.C., Bridge, J., 2014. Applying machine learning to the problem of choosing a heuristic to select the variable ordering for cylindrical algebraic decomposition, in: Intelligent Computer Mathematics, Springer International Publishing, Cham. pp. 92–107.

Iwane, H., Yanami, H., Anai, H., Yokoyama, K., 2013. An effective implementation of symbolic-numeric cylindrical algebraic decomposition for quantifier elimination. *Theoretical Computer Science* 479, 43–69. Symbolic-Numerical Algorithms.

Jia, F., Dong, Y., Liu, M., Huang, P., Ma, F., Zhang, J., 2023. Suggesting variable order for cylindrical algebraic decomposition via reinforcement learning, in: Advances in Neural Information Processing Systems, Curran Associates, Inc.. pp. 76098–76119.

Jing, R., Qian, C., Chen, C., 2024. Variable ordering selection for cylindrical algebraic decomposition via reinforcement learning. *Journal of System Science and Mathematical Science Chinese Series 0*.

Jovanovic, D., de Moura, L., 2012. Solving non-linear arithmetic, in: Automated Reasoning, Springer Berlin Heidelberg, Berlin, Heidelberg. pp. 339–354.

Kera, H., Ishihara, Y., Kambe, Y., Vaccon, T., Yokoyama, K., 2024. Learning to compute Gröbner bases. *Advances in Neural Information Processing Systems* 37, 33141–33187.

Lample, G., Charton, F., 2020. Deep learning for symbolic mathematics, in: 8th International Conference on Learning Representations, ICLR 2020, Addis Ababa, Ethiopia, April 26-30, 2020, OpenReview.net.

Lazard, D., 1994. An improved projection for cylindrical algebraic decomposition, in: Algebraic geometry and its applications: collections of papers from Shreeram S. Abhyankar's 60th birthday conference, Springer. pp. 467–476.

Lee, N., Sreenivasan, K., Lee, J.D., Lee, K., Papailiopoulos, D., 2024. Teaching arithmetic to small transformers, in: The Twelfth International Conference on Learning Representations, ICLR 2024, Vienna, Austria, May 7-11, 2024, OpenReview.net.

Lhoest, Q., Villanova del Moral, A., Jernite, Y., Thakur, A., von Platen, P., Patil, S., Chaumond, J., Drame, M., Plu, J., Tunstall, L., Davison, J., Šáško, M., Chhablani, G., Malik, B., Brandeis, S., Le Scao, T., Sanh, V., Xu, C., Patry, N., McMillan-Major, A., Schmid, P., Gugger, S., Delangue, C., Matussière, T., Debut, L., Bekman, S., Cistac, P., Goehringer, T., Mustar, V., Lagunas, F., Rush, A., Wolf, T., 2021. Datasets: A community library for natural language processing, in: Proceedings of the 2021 Conference on Empirical Methods in Natural Language Processing: System Demonstrations, Association for Computational Linguistics, Online and Punta Cana, Dominican Republic. pp. 175–184.

Li, H., Xia, B., Zhang, H., Zheng, T., 2023a. Choosing better variable orderings for cylindrical algebraic decomposition via exploiting chordal structure. *Journal of Symbolic Computation* 116, 324–344.

Li, H., Xia, B., Zhao, T., 2023b. Local search for solving satisfiability of polynomial formulas, in: Computer Aided Verification - 35th International Conference, CAV 2023, Paris, France, July 17-22, 2023, Proceedings, Part II, Springer. pp. 87–109.

Lu, P., Qiu, L., Yu, W., Welleck, S., Chang, K., 2023. A survey of deep learning for mathematical reasoning, in: Proceedings of the 61st Annual Meeting of the Association for Computational Linguistics, Association for Computational Linguistics. pp. 14605–14631.

Lu, Z., Siemer, S., Jha, P., Day, J., Manea, F., Ganesh, V., 2024. Layered and staged Monte Carlo tree search for SMT strategy synthesis, in: Proceedings of the Thirty-Third International Joint Conference on Artificial Intelligence, pp. 1907–1915.

McCallum, S., 1998. An improved projection operation for cylindrical algebraic decomposition, in: Quantifier Elimination and Cylindrical Algebraic Decomposition. Springer, pp. 242–268.

McCallum, S., Parusiński, A., Paunescu, L., 2019. Validity proof of lazard's method for CAD construction. *Journal of Symbolic Computation* 92, 52–69.

McLeish, S., Bansal, A., Stein, A., Jain, N., Kirchenbauer, J., Bartoldson, B.R., Kailkhura, B., Bhatele, A., Geiping, J., Schwarzschild, A., Goldstein, T., 2024. Transformers can do arithmetic with the right embeddings, in: *Advances in Neural Information Processing Systems*, Curran Associates, Inc.. pp. 108012–108041.

Mitchell, M., 2025. Artificial intelligence learns to reason. *Science* 387, eadw5211.

de Moura, L., Bjørner, N., 2008. Z3: An efficient SMT solver, in: *International conference on Tools and Algorithms for the Construction and Analysis of Systems*, Springer Berlin Heidelberg. pp. 337–340.

Nalbach, J., Ábrahám, E., Specht, P., Brown, C.W., Davenport, J.H., England, M., 2024. Levelwise construction of a single cylindrical algebraic cell. *Journal of Symbolic Computation* 123, 102288.

Pickering, L., del Río Almajan, T., England, M., Cohen, K., 2024a. Explainable AI insights for symbolic computation: A case study on selecting the variable ordering for cylindrical algebraic decomposition. *Journal of Symbolic Computation* 123, 102276.

Pickering, L., del Río Almajan, T., England, M., Cohen, K., 2024b. Explainable ai insights for symbolic computation: A case study on selecting the variable ordering for cylindrical algebraic decomposition. *Journal of Symbolic Computation* 123, 102276.

Quirke, P., Barez, F., 2024. Understanding addition in transformers, in: *The Twelfth International Conference on Learning Representations*.

Seidl, A., Sturm, T., 2003. A generic projection operator for partial cylindrical algebraic decomposition, in: *Proceedings of the 2003 international symposium on Symbolic and algebraic computation*, pp. 240–247.

Strzebonski, A.W., 2000. Solving systems of strict polynomial inequalities. *Journal of Symbolic Computation* 29, 471–480.

Strzebonski, A.W., 2006. Cylindrical algebraic decomposition using validated numerics. *Journal of Symbolic Computation* 41, 1021–1038.

Tarski, A., 1998. A decision method for elementary algebra and geometry, in: *Quantifier Elimination and Cylindrical Algebraic Decomposition*, Springer Vienna, Vienna. pp. 24–84.

Vaswani, A., Shazeer, N., Parmar, N., Uszkoreit, J., Jones, L., Gomez, A.N., Kaiser, L., Polosukhin, I., 2017. Attention is all you need, in: *Proceedings of the 31st International Conference on Neural Information Processing Systems*, Curran Associates Inc., Red Hook, NY, USA. p. 60006010.

Vohra, D., 2016. Apache parquet, in: *Practical Hadoop Ecosystem: A Definitive Guide to Hadoop-Related Frameworks and Tools*. Springer, pp. 325–335.

Wang, J., Chen, Y., 2023. *Introduction to Transfer Learning: Algorithms and Practice*. *Machine Learning: Foundations, Methodologies, and Applications*, Springer Singapore.

Xia, S., Li, X., Liu, Y., Wu, T., Liu, P., 2025. Evaluating mathematical reasoning beyond accuracy. *Proceedings of the AAAI Conference on Artificial Intelligence* 39, 27723–27730.

Zhu, Z., Chen, C., 2020. Variable order selection for cylindrical algebraic decomposition based on machine learning. *Journal of System Science and Mathematical Sciences (Chinese)* 40, 1492–1506.